This Project has received funding from European Commission by means of Horizon 2020,
the EU Framework Programme for Research and Innovation, under Grant Agreement no.727348

Grant Agreement No. 727348

Project Acronym:

SOCRATCES

Project title:

SOlar Calcium-looping integRAtion for Thermo-Chemical Energy Storage.

DELIVERABLE D2.1

CARBONATION KINETICS MODEL

Funding scheme:	Research and Innovation Action (RIA)		
Project Coordinator:	USE		
Start date of the project:	01.01.2018	**Duration of the project:**	36 months
Contractual delivery date:	Month 10		
Actual delivery date:	29/10/2018		
Contributing WP:	WP2		
Dissemination level:	*Public*		
Authors:	Luis Perez Maqueda (CSIC), Angeliki Lemonidou (AUTH)		
Contributors:	Jonatan Duran (CSIC), Antonio Perejon (USE), Carlos Ortiz (USE), Andy Antzara (AUTH), Athanasios Scaltsoyiannes (AUTH)		
Version:	FINAL		
Document name	**SOCRATCES_D2.1_FINAL**		

Table of contents:

INTRODUCTION 3
1. MATERIALS 5
2. ExPERIMENTAL METHODS 5
2.1. CSIC experiments 5
2.1.1. Carbonation isotherms 5
2.1.2. Multicycle activity 5
2.2. AUTH experiments 6
2.2.1. Fixed bed experiments 6
3. RESULTS AND DISCUSSION 8
3.1. CSIC experiments 8
3.2. AUTH experiments 9
4. Tables and Figures 11
4.1. Tables 11
4.2. Figures 13
5. REFERENCES 34
CONCLUSIONS 35

INTRODUCTION

This document is a public deliverable of the task 2.1 (Carbonation kinetics) included in WP2 (carbonation). The document is a report of the experimental and modelling work carried out for some of the Ca-based materials previously characterized for SOCRATCES in task 3.1 (material characterization). Thus, the objective of the work is, on one side, the proposal of a mathematical kinetic model for describing the complex carbonation reaction and, on the other, performing carbonation experiments with samples to be used in the SOCRATCES project and testing the proposed model with these experimental curves.

The materials studied are the limestones ($CaCO_3$) named GRANICARB 0.1/0.8 (Dv(50)=211µm) and OMYACARB 10 BE (Dv(50)=6.46µm) and the dolomites ($CaMg(CO_3)_2$) named DOLOMITA PPS (Dv(50)=6.70µm) and MICRODOL 1-KN (Dv(50)=6.01µm).

The influence of the type of material, particle size and carbonation temperature on the carbonation reaction rate has been studied by means of thermogravimetric analysis (TGA).

As it has been previously described in literature [1], CaO carbonation reaction takes place in two stages. Firstly, CO_2 molecules are adsorbed on the surface of the CaO particles within active centers, here represented by L:

$$\mathrm{CaO} + \underset{\theta}{\mathrm{L}} + \underset{P}{\mathrm{CO_2}} \underset{k_d}{\overset{k_a}{\rightleftarrows}} \mathrm{CaO} + \underset{1-\theta}{\mathrm{L(CO_2)}}$$

This stage (*kinetic-controlled reaction phase*) is a reversible process whose progress depends on the adsorption and desorption constants (k_a and k_d respectively), the fraction of empty active sites (represented by θ) and the CO_2 partial and absolute pressure. After the CO_2 molecules are adsorbed the reversible chemical reaction occurs, generating a $CaCO_3$ product layer on the particles surface through which CO_2 has to diffuse in order to reach the CaO core (*diffusion controlled stage*) [2-7]:

$$\mathrm{CaO} + \underset{1-\theta}{\mathrm{L(CO_2)}} \underset{k_1}{\overset{k_2}{\rightleftarrows}} \mathrm{CaCO_3} + \underset{\theta}{\mathrm{L}}$$

Reaction rates of the two steps of the kinetic-controlled reaction phase can be written as:

$$r_a = k_a \theta P - k_d (1-\theta) \quad (1)$$

$$r_2 = k_2 (1-\theta) - k_1 \theta \quad (2)$$

The pseudosteady state hypothesis [8] stablishes that adsorption rate must balance out reaction rate, which allows to define θ as [9]:

$$\theta = \frac{k_2 + k_d}{k_a P + k_d + k_1 + k_2} \quad (3)$$

According to the microscopic reversibility principle, the rate of any elementary stage must be equal to that of the inverse process (r_a=r_d=0) in order to reach equilibrium (P=P_{eq}, θ=θ_{eq}) in the overall reaction. Taking this into account, P_{eq} can be written as [9]:

$$P_{eq} = \frac{k_1}{k_2}\frac{k_d}{k_a} \quad (4)$$

In most gas-solid reactions, reaction stage is usually the rate limiting step (k_1,k_2«k_aP,k_d) [1], and therefore equation 3 and reaction rate can be rewritten as [9]:

$$\theta \approx \frac{k_d}{k_a P + k_d}$$

$$r \approx r_2 = k_2 (1-\theta) - k_1 \theta$$

From Arrhenius and Gibb's laws we have:

$$k_i = a_i e^{-E_i/RT}$$

$$\Delta G_i^0 = -RTLnK = \Delta H_i^0 - T\Delta S_i^0$$

Which allow express reaction rate as [9]:

$$r \approx a_2 e^{-E_2/RT}\left(\frac{P}{P_{eq}} - 1\right)\left(\frac{1}{\frac{P}{P_{eq}} + e^{\Delta S_2^0/R} e^{-\Delta H_2^0/RT}}\right) \quad (5)$$

Being a_2 an adjustable preexponential factor, R the ideal gas constant (8.31 J/K·mol) and E_2 the carbonation activation energy (20 kJ/mol) [9-11]. ΔS_2^0 and ΔH_2^0 are the standard entropy and enthalpy of the reaction, which are calculated as [9-13]

$$\Delta S_2^0 = \Delta S_r^0 - \Delta S_a^0 = -160 - (-92) = -68\ \mathrm{J/K \cdot mol}$$

$$\Delta H_2^0 = E_2 - E_1 = 20 - 180 = -160\ \mathrm{kJ/mol}$$

P_{eq} values, which will be used in equation 5, are calculated from [9]:

$$P_{eq} = Ae^{-\alpha/T} \quad (6)$$

Where $A = 4.083 \cdot 10^7 \mathrm{atm}$ and $\alpha = 20474\ \mathrm{K}$. The values for reaction enthalpies, entropies, and activation energies required for the calculation of the reaction rate were acquired from thermochemical data [9] and are summarized in Table 5.

As it is inferred from equation 5, temperature and pressure have a big influence in reaction progress. Particles heterogeneities are also relevant as far as they make some active centres more accessible than others. Taking these constraints into account, reaction progress can be defined as:

$$\frac{dX}{dt} = f(X)r(T,P) \quad (7)$$

Where $f(X)$ is a mechanistic function that takes into account material's morphology and $r(T,P)$ the reaction rate, which will be calculated from equation 5. A Prout-Tompkins reaction model will be assumed, $f(X) = X(1-X)$ [14]. The reaction progress (X) has been calculated from the thermogravimetric experimental data of CaO carbonation according to equation (8):

$$X = \frac{m\% - m\%_0}{m\%_f - m\%_0} \quad (8)$$

being $m\%_0$ the initial mass%, $m\%_f$ the final mass% and $m\%$ the sample mass at an instant time t.

As it was previously mentioned, CO_2 molecules have to diffuse through the $CaCO_3$ product layer. Diffusion through this layer is hindered for the gas molecules, and when the layer reaches a critical thickness, reaction progress is governed by CO_2 diffusion instead of chemical reaction. Therefore, it is reasonable to rewrite equation 7 as [9]:

$$\frac{dX}{dt} = X\left(1 - \frac{X}{X_k}\right)r(T,P) \leftrightarrow X(t) = \frac{X_k}{1 + e^{-r(t-t_0)}} \quad (9)$$

Where X_k is the conversion value after which reaction is governed by CO_2 diffusion and t_0 the instant at which the kinetic-controlled reaction phase is exactly at its half conversion degree.

When several calcination/carbonation cycles are performed, sintering-induced CaO deactivation causes incomplete conversion of CaO, which progressively decreases until a certain residual value, X_R. The speed at which this decay progress can be estimated from the

deactivation constant, k. This two parameters can be obtained by fitting the experimental conversion values with equation 10 [15]:

$$X_N = X_R + \frac{X_1}{k(N-1) + \left(1 - \frac{X_r}{X_1}\right)^{-1}} \quad (10)$$

Where N is the cycle number and X_N the effective conversion at the N^{th} cycle. X_N is calculated as:

$$X_N = \frac{m_{carb\ N} - m_{cal\ N}}{m_{cal\ N}} \frac{WCaO}{WCO_2} \quad (11)$$

Where $m_{cal\ N}$ and $m_{carb\ N}$ are the sample masses before and after carbonation at the N^{th} cycle. W_{CaO} and W_{CO2} are the molar masses of CaO and CO_2, respectively. Note that X_N and X(t) are not the same parameters since the latter is equivalent to the term α(t), typically employed in kinetic studies. Equation 10 cannot be applied to dolomites multicycle activity because the deactivation constants for these materials are too low.

1. MATERIALS

The limestones and dolomites were selected for this study from the samples provided by the suppliers OMYA and TALJEDI, considering their purity and particle size. Relevant parameters of the samples used for the experiments are shown in table 1. From a chemical and structural point of view, all the samples tested by CSIC are quite pure and show a single crystalline phase (calcite in case of limestones GRANICARB 0.1/0.8 and OMYACARB 10 BE (both from OMYA) and dolomite for DOLOMITA PPS (TALJEDI) and MICRODOL 1-KN (OMYA)).

2. EXPERIMENTAL METHODS

2.1. CSIC experiments

2.1.1. Carbonation isotherms

The kinetics of carbonation reaction was studied by CSIC using a Q5000IR thermogravimetric analyzer (TA Instruments) provided with a high sensitivity balance, a fast furnace heated by IR lamps and a small volume reactor that allows a very rapid change of atmosphere.

Carbonation was carried out at different temperatures in both pure CO_2 and 70%vol. CO_2:30%vol. He atmosphere. The samples were initially calcined under pure He and then the temperature was changed to the selected temperature, which was stabilized for 5 minutes. Then, the atmosphere was modified from pure He to either pure CO_2 or 70% vol. CO_2. An example of this kind of experiments is shown in Figure 1.

2.1.2. Multicycle activity

The multicycle activity of the samples was also evaluated using the same TG analyzer employed for carbonation isotherms. Carbonation/calcination cycles consisted of heating the samples under 70% vol. concentration of CO_2 or pure CO_2 to produce the calcination (thermal decomposition of the calcium carbonate to obtain CaO) followed by a change in temperature under the same atmosphere to carbonate the material (reaction of CaO with CO_2 to obtain $CaCO_3$).

The temperatures of calcination and carbonation were selected in each case considering the corresponding equilibrium temperatures (895°C and 870°C for pure CO_2 and 70% vol. CO_2

concentration, respectively) and that fast carbonation and calcination reactions are needed in the practical application. Figures 26 and 27 show the temperature profiles employed and typical mass-time curves obtained for both experimental conditions.

Deactivation constants and residual conversion values of the samples were obtained by fitting the experimental data to equation 10. The fittings are shown in Figure 32 and the k and X_R values are presented in Table 4.

2.1.2.1. Carbonation and calcination under 100%vol. CO_2 atmosphere

The experiments started with a calcination stage, consisted of heating the sample from room temperature to 950°C at 300°C/min followed by a 5-minute isotherm. Then, the temperature was decreased at 300°C/min to 850°C and maintained for 5 minutes to perform carbonation under pure CO_2. After carbonation, the sample was calcined again by increasing the temperature (300°C/min) to 950°C. The calcination stage was maintained for 5 min to achieve full CaO regeneration. Carbonation was carried out again by decreasing the temperature at 300°C/min to 850°C after which a new cycle was started. A total of 10 calcination/carbonation cycles were performed.

2.1.2.2. Carbonation and calcination under 70%vol. CO_2 atmosphere

The experiments started with a calcination stage, consisted of heating the sample from room temperature to 920°C at 300°C/min followed by a 5-minute isotherm. Then, the temperature was decreased at a rate of 300°C/min to 800°C and maintained for 5 minutes to perform carbonation. After carbonation, the sample was calcined again by increasing the temperature at 300°C/min to 920°C followed by a new 5-minute isotherm. Then, the temperature was decreased for a new carbonation stage at 800°C. A total of 10 carbonation/calcination cycles were performed.

2.2. AUTH experiments

2.2.1. Fixed bed experiments

2.2.1.1. Unit description

The kinetic measurements for the carbonation reactor were performed in a bench scale laboratory unit near atmospheric pressure equipped with a fixed bed reactor (Figure 33). The continuous flow unit which operates near atmospheric pressure consists of the gas feed inlet section, the reactor and the product analysis section. The incoming gases are controlled by mass flow controllers and are pre-mixed before entering the reactor. A fixed bed quartz reactor (10mm internal diameter), equipped with a coaxial thermocouple for temperature monitoring, is used for the testing. The reactor is heated electrically by a tubular furnace, with three independently controlled temperature zones. The hot gases exiting the reactor are cooled down to room temperature and continuously analyzed by a mass spectrometer (MS) (Omnistar ^{TM} GSD 320, PFEIFFER).

2.2.1.2. Experimental protocol

The sorbent materials were sieved in the range of $45 < d_p < 75\mu m$ and about 100 mg mixed with 1.5 gr of quartz with particle size of $100 < d_p < 180\mu m$ were loaded in the reactor. The reactor was heated (heating rate of 20°C/min) up to the carbonation temperature (e.g. 880 °C) under N_2 flow of 200cc/min, so that full calcination is taking place (pretreatment). When

carbonation temperature was reached, carbonation initiated by switching the flow from pure N_2 to 600cc/min of CO_2 (containing 2%vol. Ar used as an internal standard). The carbonation stage was carried out for 3 mins isothermally. Given that the Ar flow was constant, the flow ratio of CO_2/Ar decreased when carbonation reaction was taking place. The flow changes were detected by the mass spectrometer. Temperature in the reactor was also recorded during the whole procedure. Subsequently, a flow of 200 cc/min of pure N_2 was introduced into the reactor to calcine the sorbent isothermally for 3 mins and the cycle was repeated. The above procedure (one cycle) is presented schematically in Figure 34.

3. RESULTS AND DISCUSSION

3.1. CSIC experiments

Tables 2 and 3 list the reaction rate values of carbonation for the different isotherms performed under 70% vol. CO_2 concentration and pure CO_2 respectively. It is observed that reaction rates decrease as carbonation temperatures approach the equilibrium temperature, as expected taking into account the chemical equilibrium constraints. The equilibrium temperatures are 895°C and 870°C for pure CO_2 and 70% vol. CO_2 concentration, respectively.

The trend obtained for the reaction rates of carbonation can be clearly observed in the X vs time plots (Figures 2-21). For the carbonation experiments carried out in the temperature range 650°C-800°C (Figures 3, 6, 9, 12, 15 and 19) an overshoot in the mass signal is observed. This effect is attributed to the very fast carbonation reaction that takes place at these temperatures, which causes a rapid increase in the sample temperature due to the exothermicity of the process. Therefore, the real sample temperature should not follow the preset program during the carbonation process and it might cause a small destabilization of the mass signal that produces the bump in the TG trace. This effect seems to be more pronounced at the lowest temperatures and it is less relevant for GRANICARB 0.1/0.8 sample since the particles size of this limestone is relatively large and carbonation rate is much lower than that of OMYACARB 10 BE. For DOLOMITA PPS, the effect is more pronounced since carbonation reaction takes place faster for dolomites than for limestones for similar particle size distributions.

Due to this phenomenon, deviations of the experimental values of reaction rate from that predicted by the model (Figures 22-25) are obtained.

Anyway, the kinetic-controlled reaction phase of carbonation is well fitted by equation 9 (Figures 2-21) and therefore the reaction rate values obtained are representative of the experimental data. From Figures 22-25, it can be concluded that at the same temperature, carbonation reaction is faster as CO_2 concentration increases, which is in agreement with thermodynamic constrains.

Regarding the multicycle activity of the samples (Figure 32), the effective conversion decreases with the cycle number [2-5], due to CaO sintering that is promoted by the presence of CO_2 [6, 7]. The multicycle activity of the limestones is higher as the median particle size decreases. Thus, X_1 and X_R values are higher for OMYACARB 10 BE than for GRANICARB 0.1/0.8. On the other hand, similar values of X_1, X_R and k are obtained for the samples when cycled under pure CO_2 and 70%vol. CO_2. Hence, it can be stablished that the effect of particle size on CO_2 uptake is much more relevant than that of the experimental conditions employed to perform the calcination/carbonation cycles.

Note that the samples have been tested under two different CO_2 concentrations and also employing different temperatures for carbonation and calcination depending on CO_2 concentration. A slightly better performance of the samples is obtained when cycled under 70%vol. CO_2 concentration, with carbonations at 800°C and calcinations at 920°C.

One of the dolomites tested in this study (DOLOMITA PPS) presents a higher multicycle performance (X_{eff}) than the limestones (Figure 32). This behaviour is related to the presence in the material of MgO grains after the first calcination that are inert to carbonation in the experimental conditions employed. These grains prevent CaO sintering in the first cycles, but segregate from the CaO grains as the number of cycles increases and from the fourth cycle the effective conversion decreases. The X_1 and X_{10} values (Table 4) show that although the initial effective conversion for dolomite is lower than for limestone (the maximum X_N achievable for dolomite is 0.58), the long-term effective conversion is much higher.

3.2. AUTH experiments

In Figures 35 and 36, carbonation conversion is plotted as a function of time at different carbonation temperatures for a limestone (GRANICARB 0.1/0.8 (OMYA)) and a dolomite (MICRODOL 1-KN (OMYA)) sample respectively. As can be observed, in all cases the carbonation reaction proceeds via a typical two-stage mechanism. As it was described in the introduction of this document, in the first stage (fast regime) the rate determining step of carbonation is the rapidly progressing surface reaction between CO_2 and CaO at the interface of the product layer and the unreacted CaO core. As the formation of $CaCO_3$ proceeds, the overall CO_2 capture process is governed by diffusion of CO_2 through the $CaCO_3$ product layer. Carbonation rate during the fast kinetically-controlled regime decreases at higher temperatures. As the reaction approaches equilibrium temperature for the studied CO_2 partial pressure it is governed mainly by thermodynamics limitations, resulting at lower reaction rates. It is important to note however that in all cases an adequate conversion of the material is achieved in very short times (less than 10 seconds), comparable to the residence time of the particles in a drop-down tube reactor.

Although a highly diluted material bed was used, as shown in Figure 37 it was not possible to maintain a constant temperature in the reactor due to the strong exothermicity of carbonation reaction of CaO with CO_2. When and initial temperature of 880°C was applied, the reaction proceeded with very fast rate, even after 10 sorption/desorption cycles when the material was deactivated, a residual temperature increase of around 5°C still remains. In all cases, the maximum carbonation rate was observed at ≈2 seconds reaction time. A milder temperature increase was observed when the temperature of the reactor was set at 890 and 900°C which are closer to the equilibrium temperature for a pure CO_2 stream and an operating pressure of ≈1.7 bar during the first cycles, with the ΔT observed in the reactor due to the exothermicity of the carbonation stabilizing in similar values for each experiment after ≈10 cycles (Figure 37b).

The performance of the two different materials used (OMYA GRANICARB 0.1/0.8 (45 -75 μm) and OMYA MICRODOL 1-KN (45 -75 μm)) under the same reaction conditions is presented in Figure 38. Dolomite exhibited higher reaction rates than limestone, probably due to the larger surface area. In addition, MgO content provide an increased sintering resistance to the material compared to limestone, achieving a much higher final conversion of >80% after 5 carbonation/calcination cycles (Figure 39). This gives compensation for the lower CaO concentration (≈67% wt. after calcination).

The modified Prout-Tompkins (P-T) kinetic described in the introduction was used to describe the evolution of the carbonation conversion versus time in the fixed bed experiments performed at AUTH. The effect of temperature for values close to equilibrium at the operating pressure during carbonation stage is shown in Figure 40. The modelling results are in a very good agreement with the experimental data of CaO fractional conversion evolution as a function of time, showing that a typical sigmoidal curve of gas-solid reactions can be fitted adequately by the used Prout−Tompkins function (equation 9). Notice that fractional conversion $\alpha(t)$ is equal to $X(t)/X_k$, where X_k is the conversion achieved considering only the kinetically controlled regime. The values of X_k were obtained from the experimental data (Figure 35) and are presented in Table 6. The results of the fitting process (r and t_0 values) are summarized in Table 7. As shown, the obtained values of the rate of the carbonation reaction are more than one order of magnitude higher compared to the results obtained using a TGA apparatus by Ortiz et al. [9], where the reaction time was much higher at similar temperatures (≈20 min compared to few seconds in the fixed bed reactor). The pre-exponential factor of the carbonation reaction can be calculated using equation 5 and the data from Table 5. The values of a_2 for the three temperatures are summarized in Table 8. As can be seen from these values, the pre-exponential factor values are very close (≈75000 s^{-1}) showing the validity of equation 5. Ortiz et al. [9] calculated a_2 equal to 1160 s^{-1}, based on TGA experiments. The reaction time

needed for carbonation in a TGA apparatus is of the order of a few minutes while in a fixed bed needs only a few seconds, resulting in such a large a_2 value).

In order to model the deactivation rate in CaO conversion during multiple cycles equation 10 was used. Effective kinetic parameter estimation was performed under dedicated optimization algorithms of Matlab/Mathworks. The modelling of the deactivation rate of the limestone material during multiple sorption/desorption cycles is presented in Figure 41. The value of the residual carbonation conversion X_r was set at ≈8%, typically referred in literature. As shown, the used empirical equation can satisfactorily describe the performance of the material in multiple cycles. It can be observed that the experimental data are distributed on both sides close to the fitting curve, indicating the adequacy of the used model.

4. TABLES AND FIGURES

4.1. Tables

Table 1. – Purity (from XRD measurements), particle size distribution (μm) and S_{BET} (m^2/g) of CSIC samples.

SAMPLE	Purity	S_{BET}	Dv(10)	Dv(50)	Dv(90)	D[3;2]	D[4;3]
OMYACARB 10 BE	Pure calcite	1.6	2.50	6.46	13.5	4.85	7.30
GRANICARB 0.1/0.8	Pure calcite	0.4	2.83	211	489	10.6	225
DOLOMITA PPS	Pure dolomite	1.3	1.06	6.70	32.1	3.12	12.4
MICRODOL 1-KN	Pure dolomite	2.8	0.889	2.75	7.44	2.95	6.96

Table 2. – Reaction rates (min^{-1}) of carbonation at different temperatures under 70%vol. CO_2.

TEMPERATURE	OMYACARB 10 BE	GRANICARB 0.1/0.8	DOLOMITA PPS
860°C	0.06	0.02	0.04
850°C	0.94	1.71	1.24
840°C	-	6.30	-
830°C	-	7.31	-
825°C	6.60	7.27	9.52
810°C	-	14.62	-
800°C	15.85	18.63	15.93
750°C	35.25	18.79	45.54
700°C	52.64	18.86	61.68
650°C	68.30	31.98	86.04

Table 3. – Reaction rates (min^{-1}) of carbonation at different temperatures under 100% CO_2.

TEMPERATURE	OMYACARB 10 BE	GRANICARB 0.1/0.8	DOLOMITA PPS
890°C	-	1.74	-
885°C	-	3.01	-
880°C	-	4.13	-
875°C	-	4.73	-
870°C	6.91	8.38	6.02
865°C	-	6.65	-
860°C		8.57	
850°C	10.72	9.33	14.83
825°C	13.94	-	30.47
800°C	15.92	23.29	39.76
750°C	17.53	22.65	62.59
700°C	17.48	48.96	102.48
650°C	16.71	17.04	100.95

Table 4. – Deactivation constant, initial and residual conversion values for the cycled limestones and dolomite by CSIC.

SAMPLE	%CO_2	X_1	X_{10}	X_R	k
OMYACARB 10 BE	70	0.73	0.29	0.18	0.56
	100	0.71	0.28	0.19	0.58
GRANICARB 0.1/0.8	70	0.69	0.19	0.08	0.50
	100	0.65	0.17	0.06	0.52
DOLOMITA PPS	70	0.56	0.41	-	-
	100	0.56	0.40	-	-

Table 5. – CO_2 Values of Enthalpy–Entropy changes in the chemical decomposition and desorption stages and activation energies.

Parameter	Value
ΔH^0_r (kJ/mol)	180
ΔH^0_1 (kJ/mol)	160
ΔH^0_d (kJ/mol)	20
E_d (kJ/mol)	20
E_a (kJ/mol)	20
E_1 (kJ/mol)	180
ΔS^0_r (kJ/(mol K))	0.16
ΔS^0_1 (kJ/(molK))	0.068
ΔS^0_d (kJ/(molK))	0.092
R (kJ/(molK))	0.008314
A (atm)	40830000
α (K)	20474

Table 6. – Values of X_k introduced in the P-T model (equation 9) for carbonation under pure CO_2.

T (°C)	880	890	900
X_k	22.0	13.3	8.2

Table 7. – Parameters derived from the P-T model (equation 9) for carbonation under pure CO_2.

T (°C)	880	890	900
r (1/s)	2.07	1.80	1.46
t_0 (s)	1.577	1.515	1.916

Table 8. – Values of a_2 calculated from equation 5 for carbonation under pure CO_2 at 880, 890 and 900°C.

T (°C)	880	890	900
a_2 (1/s)	74100	74900	75000

4.2. Figures

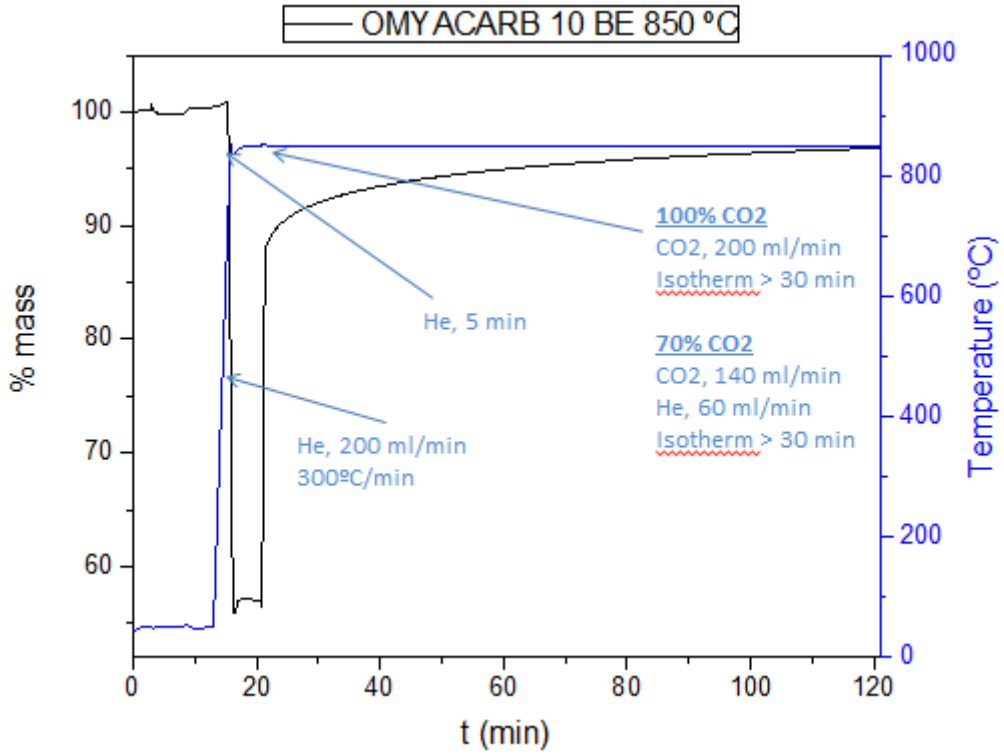

Figure 1. – OMYACARB 10 BE thermogram showing the time evolution of temperature and mass for a typical isothermal experiment of carbonation. The different stages of the experiment are shown in the figure.

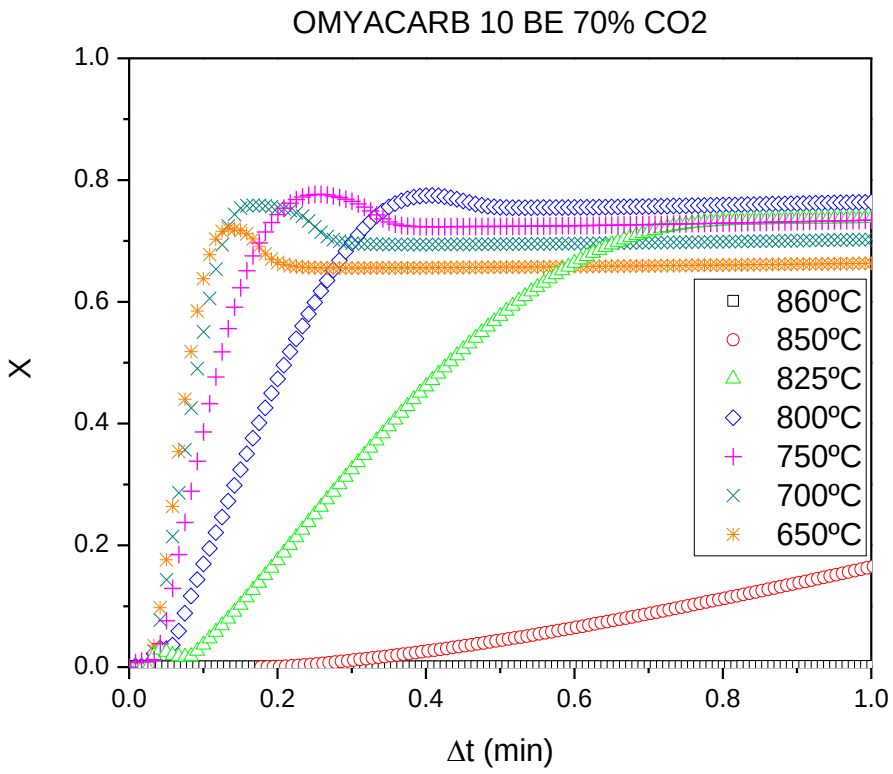

Figure 2. – X vs time plot for OMYACARB 10 BE. Carbonation was performed at different temperatures under 70%vol. CO_2.

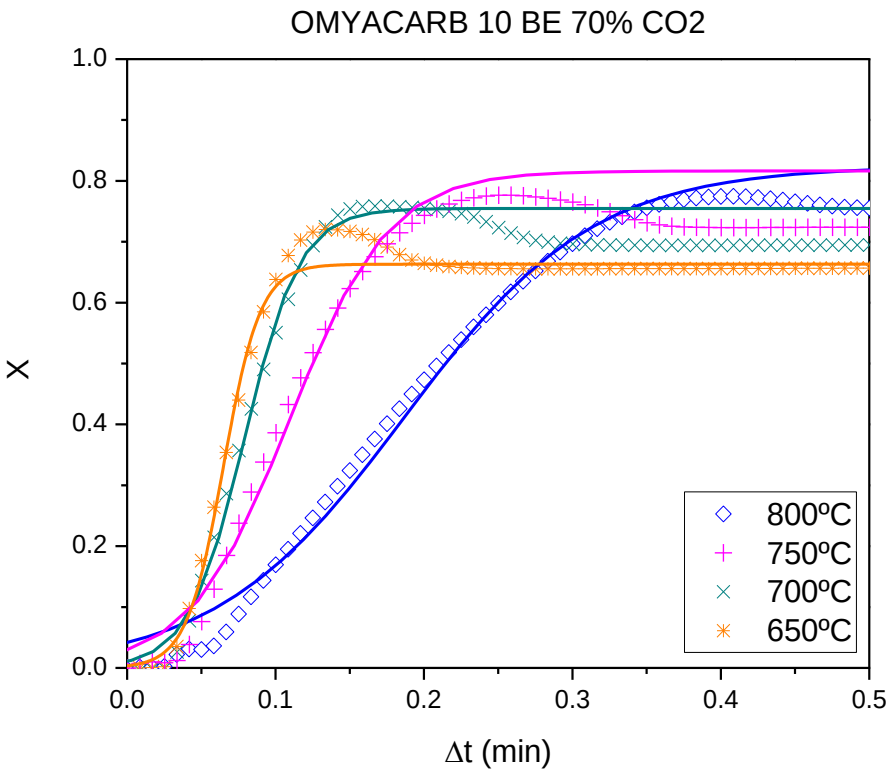

Figure 3. – X vs time plot for OMYACARB 10 BE carbonated at 650°C, 700°C, 750°C and 800°C under 70%vol. CO_2. The symbols correspond to experimental data and the solid lines correspond to the fit to equation 9.

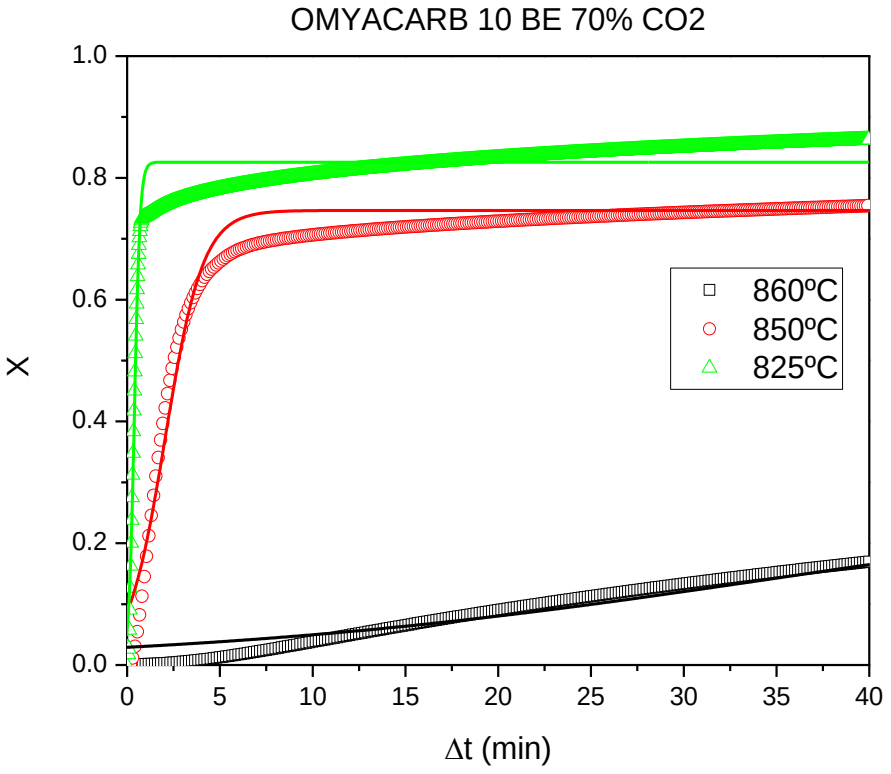

Figure 4. – X vs time plot for OMYACARB 10 BE carbonated at 825°C, 850°C and 860°C under 70%vol. CO_2. The symbols correspond to experimental data and the solid lines correspond to the fit to equation 9.

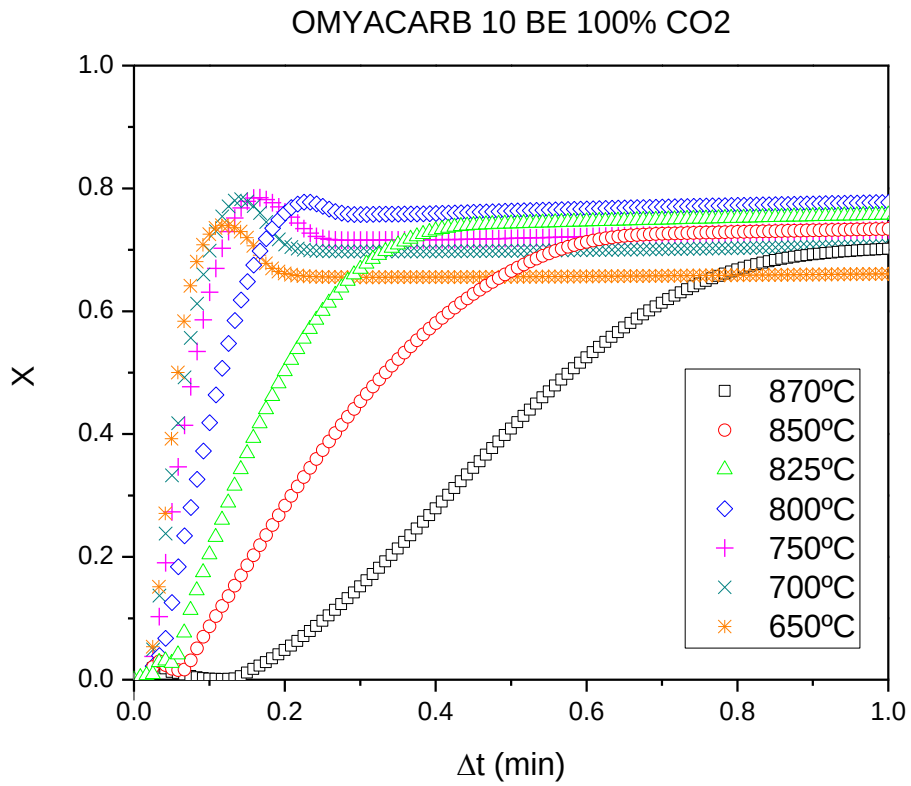

Figure 5. – X vs time plot for OMYACARB 10 BE. Carbonation was performed at different temperatures under pure CO_2.

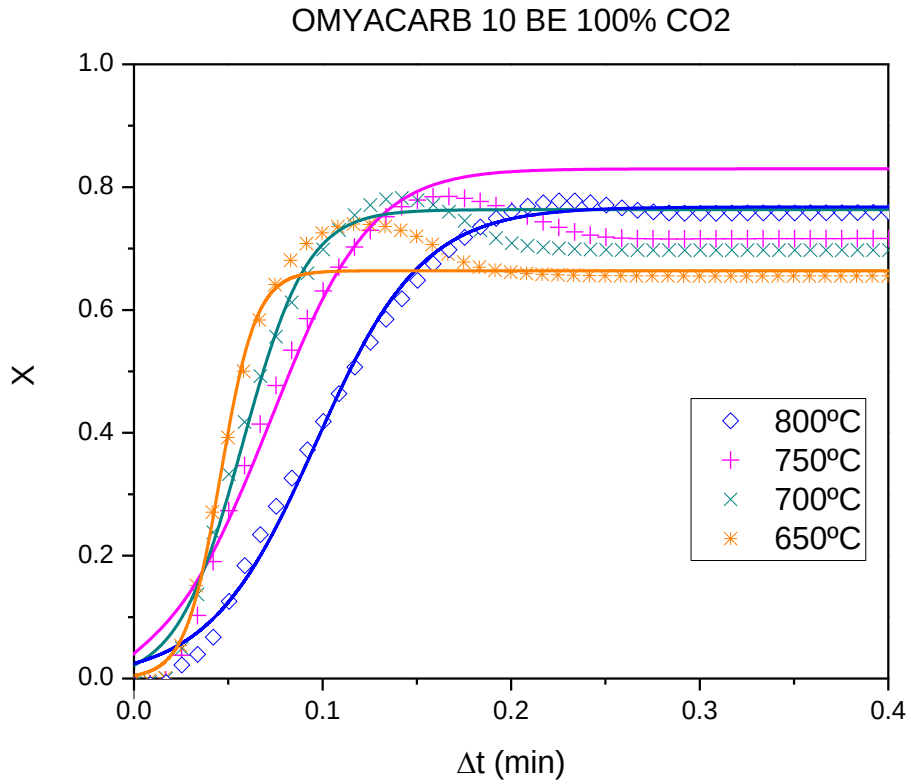

Figure 6. – X vs time plot for OMYACARB 10 BE carbonated at 650°C, 700°C, 750°C and 800°C under pure CO_2. The symbols correspond to experimental data and the solid lines correspond to the fit to equation 9.

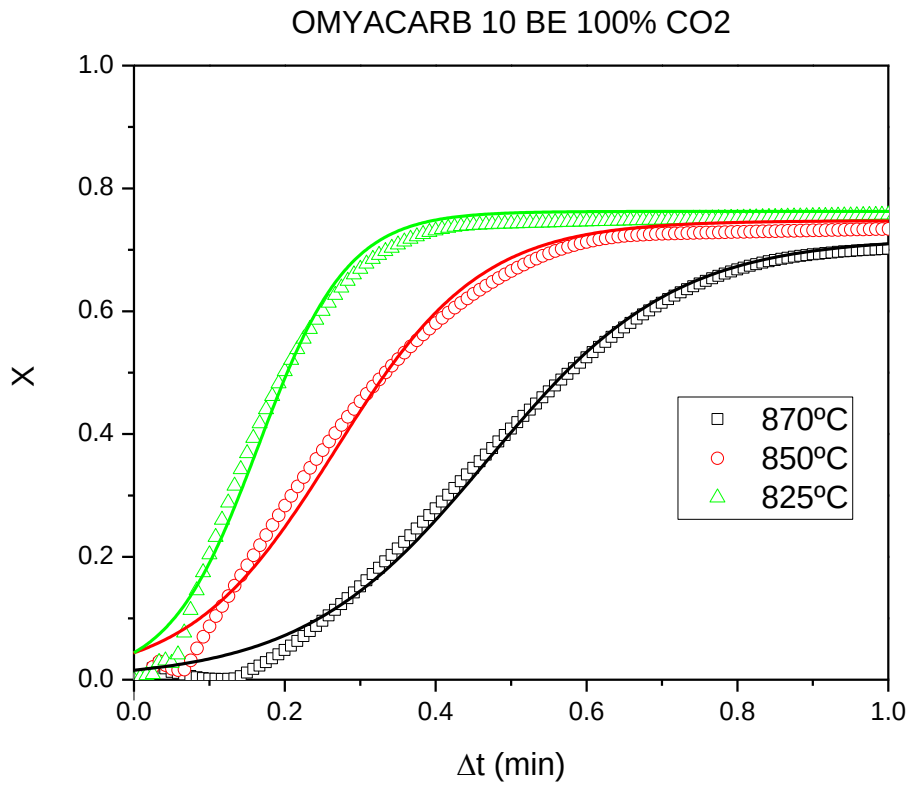

Figure 7. – X vs time plot for OMYACARB 10 BE carbonated at 825°C, 850°C and 870°C under pure CO_2. The symbols correspond to experimental data and the solid lines correspond to the fit to equation 9.

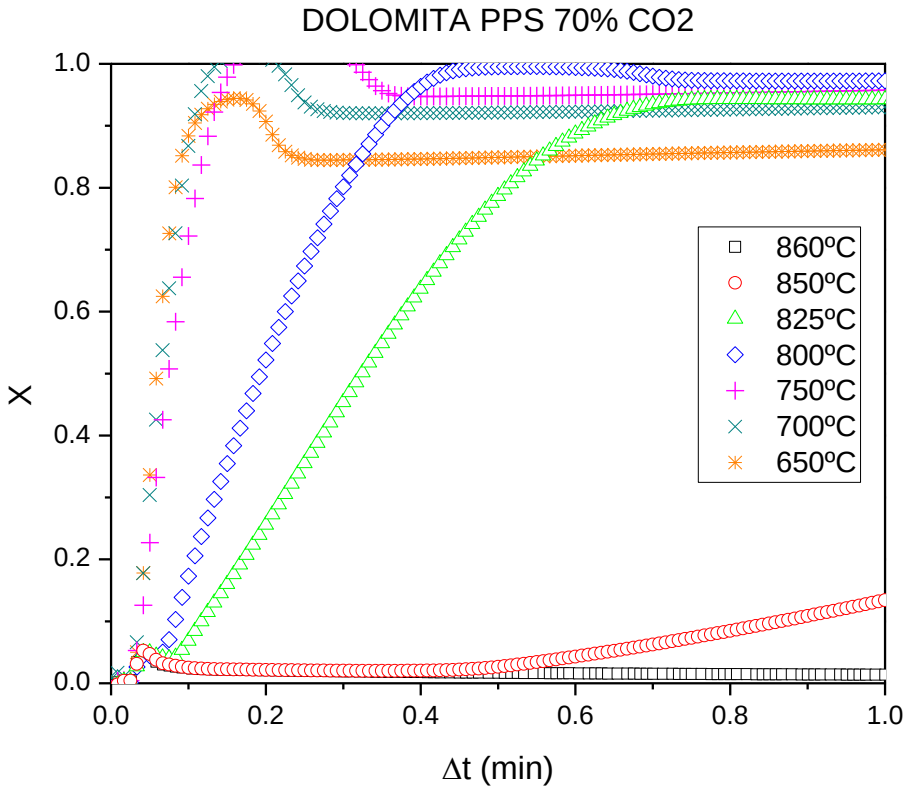

Figure 8. – X vs time plot for DOLOMITA PPS. Carbonation was performed at different temperatures under 70%vol. CO_2.

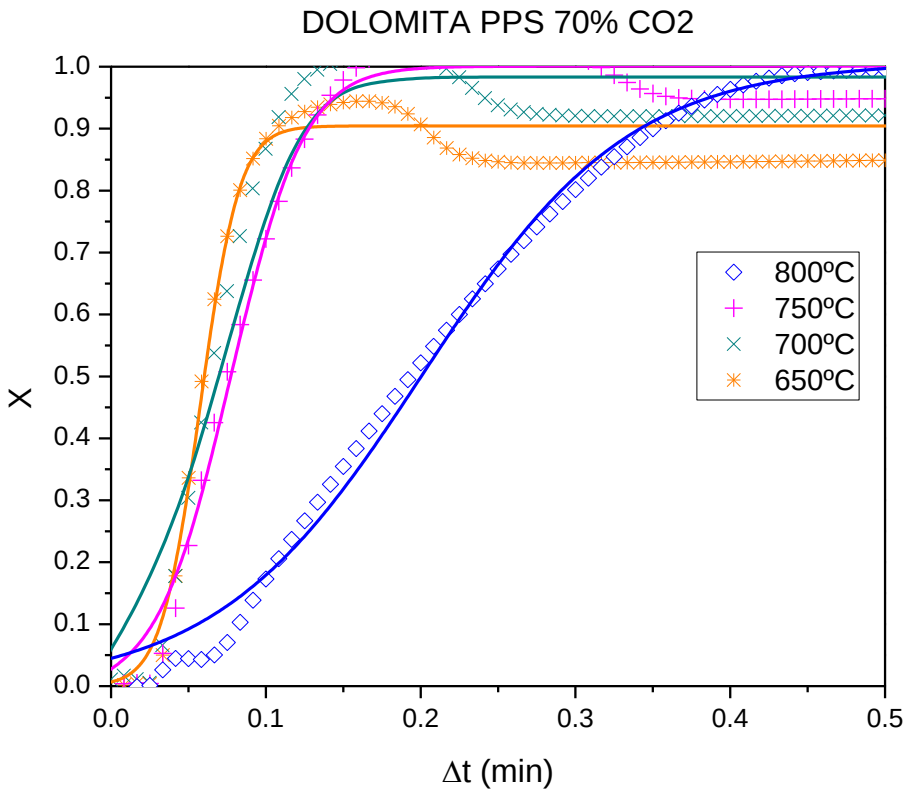

Figure 9. – X vs time plot for DOLOMITA PPS carbonated at 650°C, 700°C, 750°C and 800°C under 70%vol. CO_2. The symbols correspond to experimental data and the solid lines correspond to the fit to equation 9.

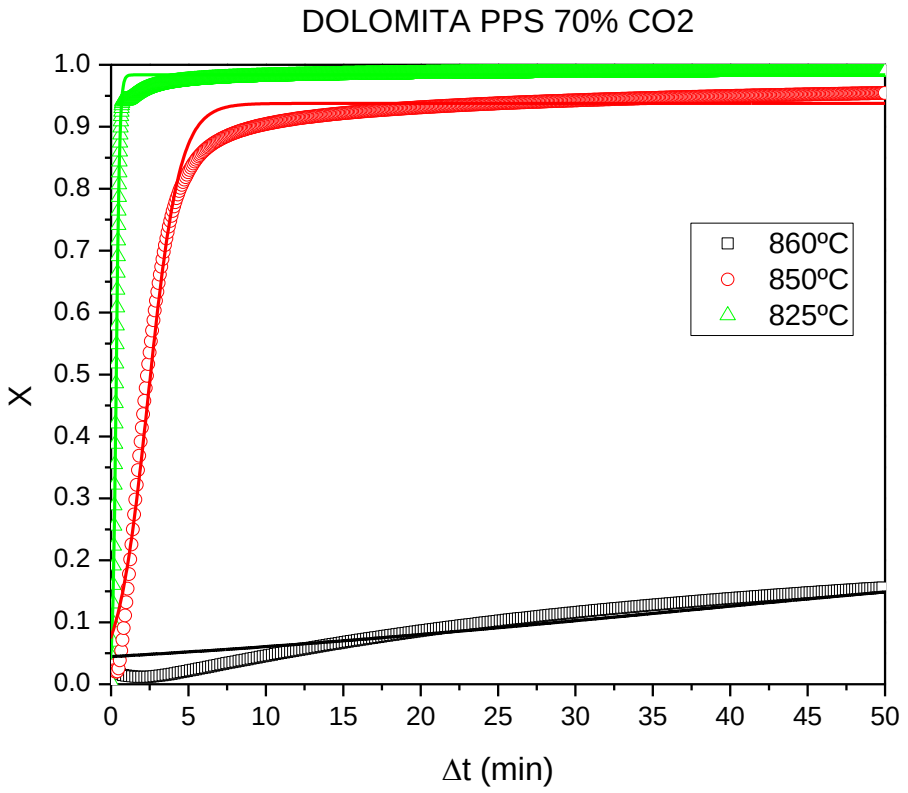

Figure 10. – X vs time plot for DOLOMITA PPS carbonated at 825º, 850°C and 860°C under 70%vol. CO_2. The symbols correspond to experimental data and the solid lines correspond to the fit to equation 9.

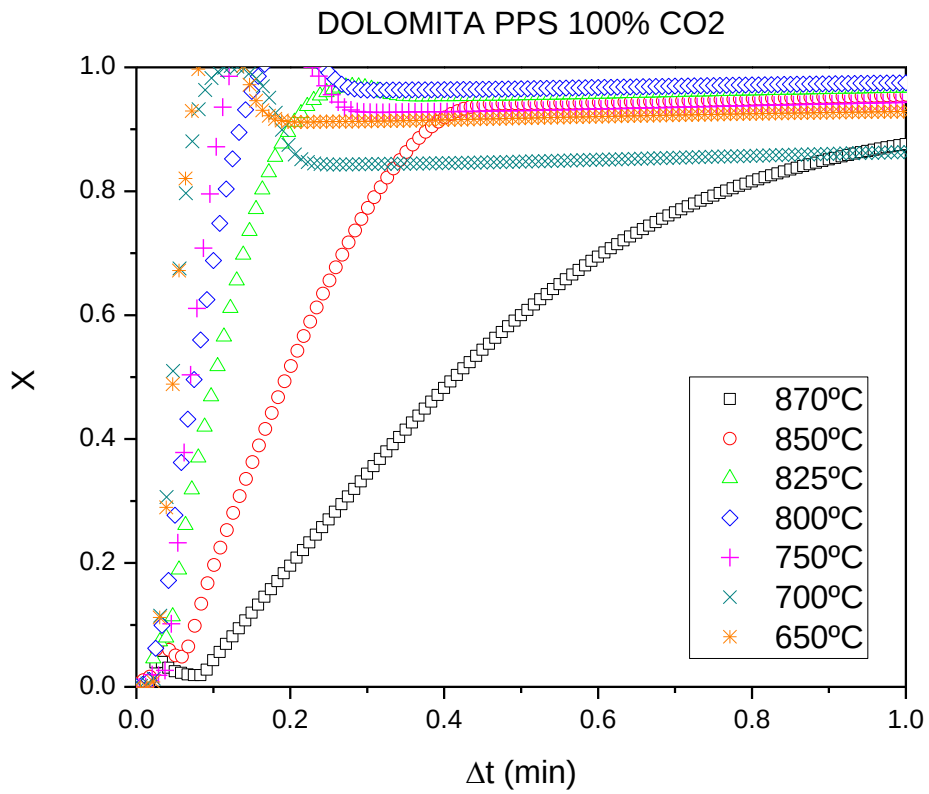

Figure 11. – X vs time plot for DOLOMITA PPS. Carbonation was performed at different temperatures under pure CO_2.

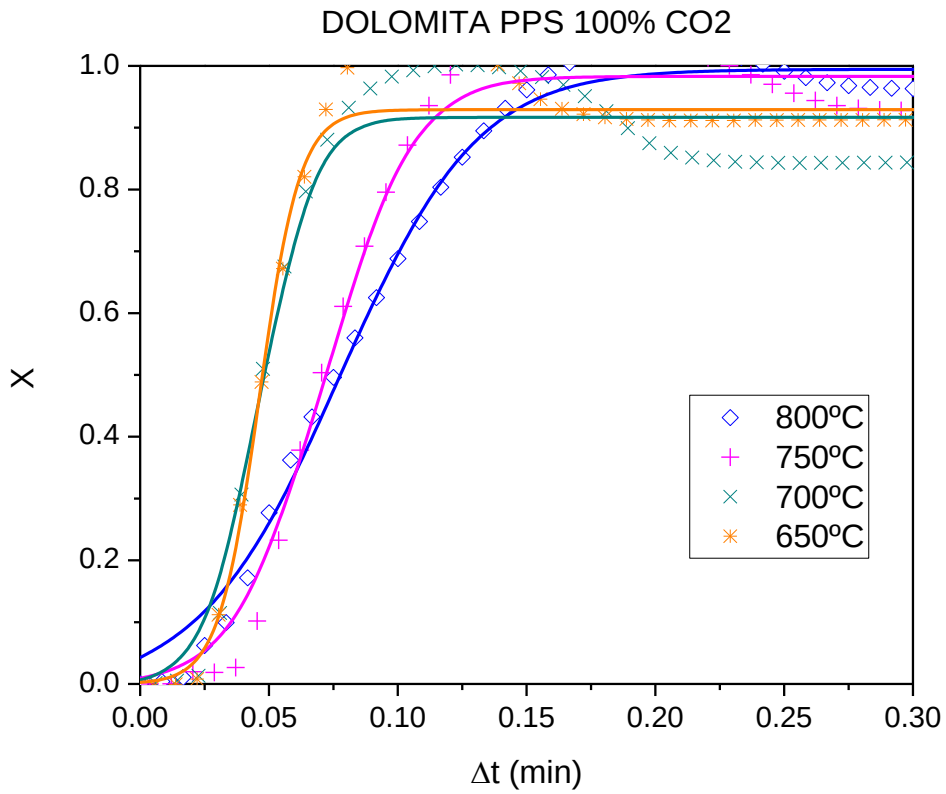

Figure 12. – X vs time plot for DOLOMITA PPS carbonated at 650°C, 700°C, 750°C and 800°C under pure CO_2. The symbols correspond to experimental data and the solid lines correspond to the fit to equation 9.

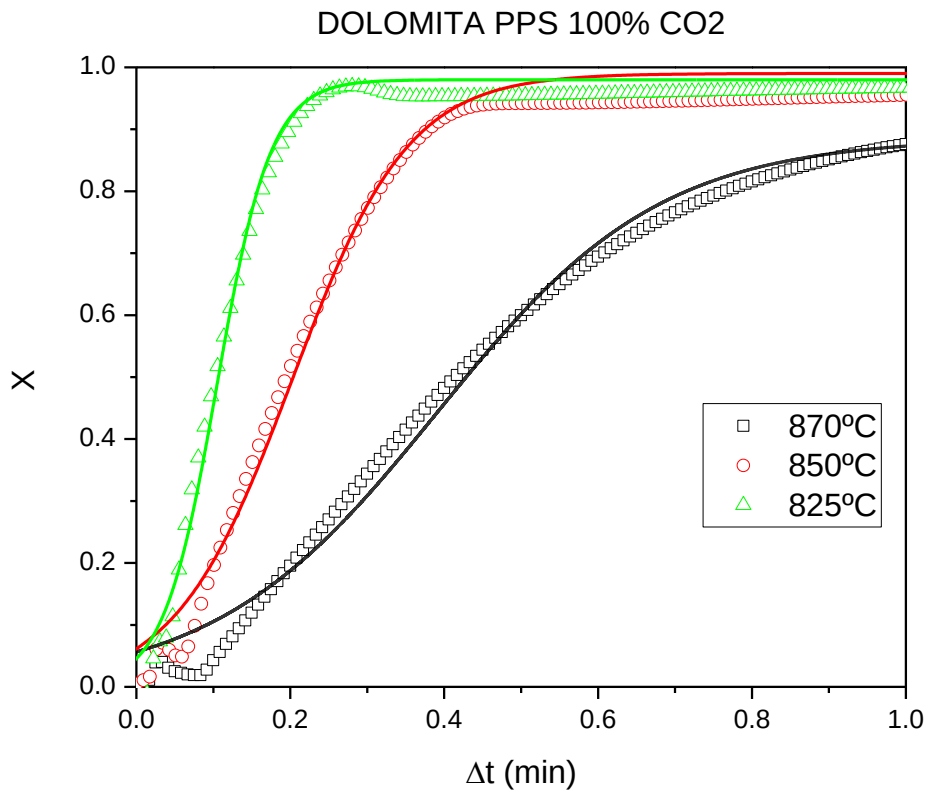

Figure 13. – X vs time plot for DOLOMITA PPS carbonated at 825°C, 850°C and 870°C under pure CO_2. The symbols correspond to experimental data and the solid lines correspond to the fit to equation 9.

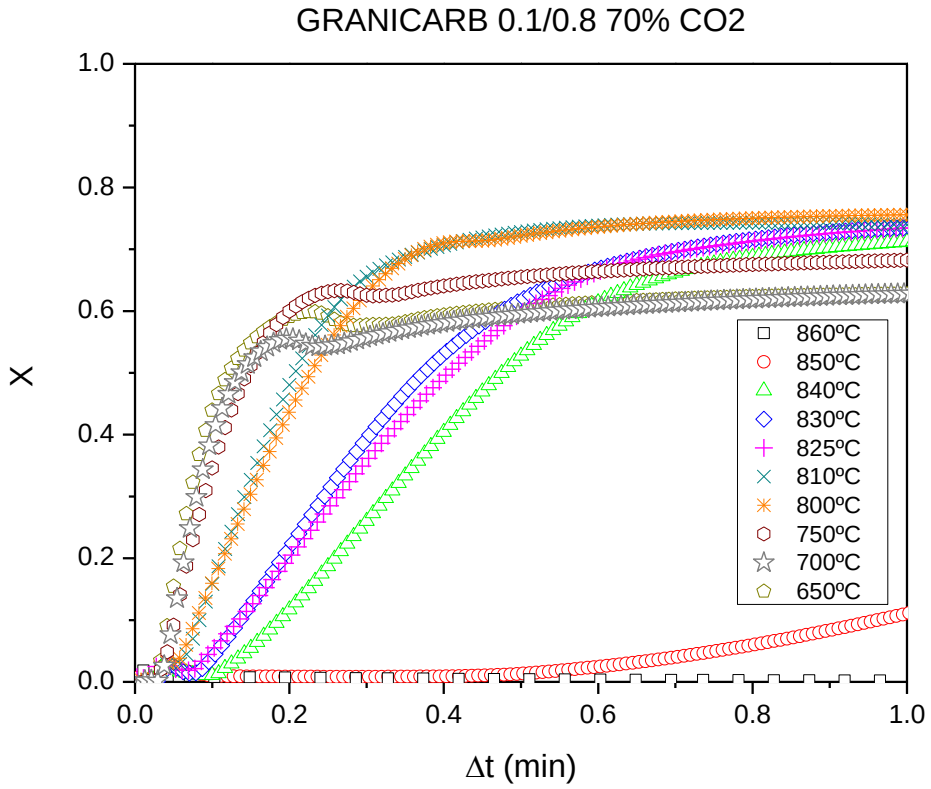

Figure 14. – X vs time plot for GRANICARB 0.1/0.8. Carbonation was performed at different temperatures under 70%vol. CO_2.

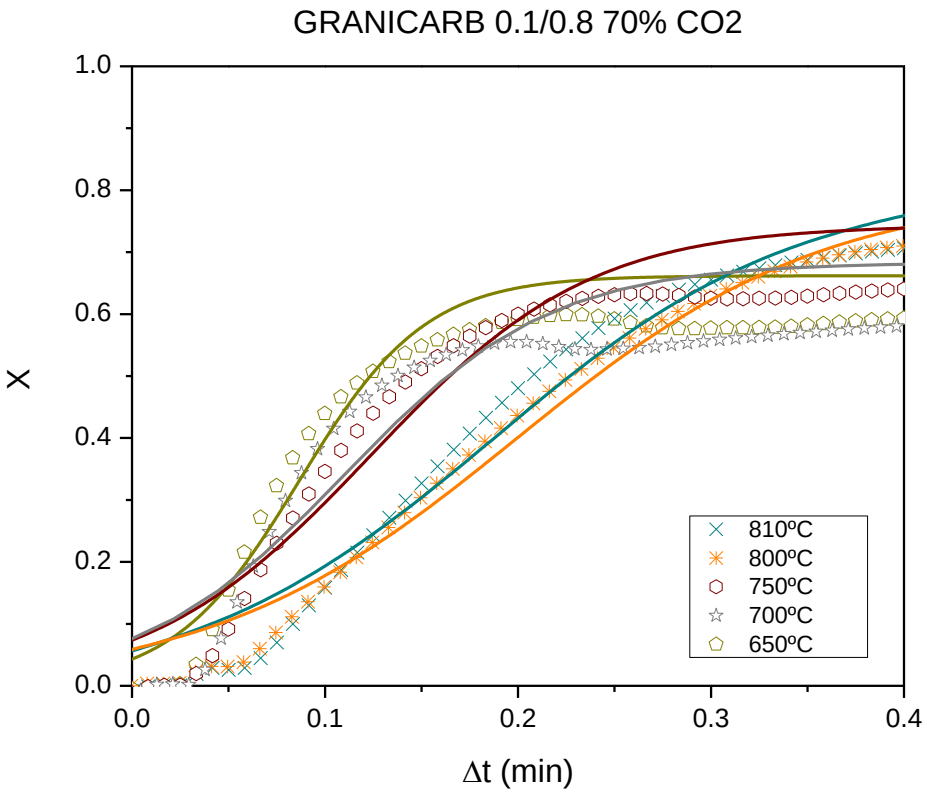

Figure 15. – X vs time plot for GRANICARB 0.1/0.8 carbonated at 650°C, 700°C, 750°C, 800°C and 810°C under 70%vol. CO_2. The symbols correspond to experimental data and the solid lines correspond to the fit to equation 9.

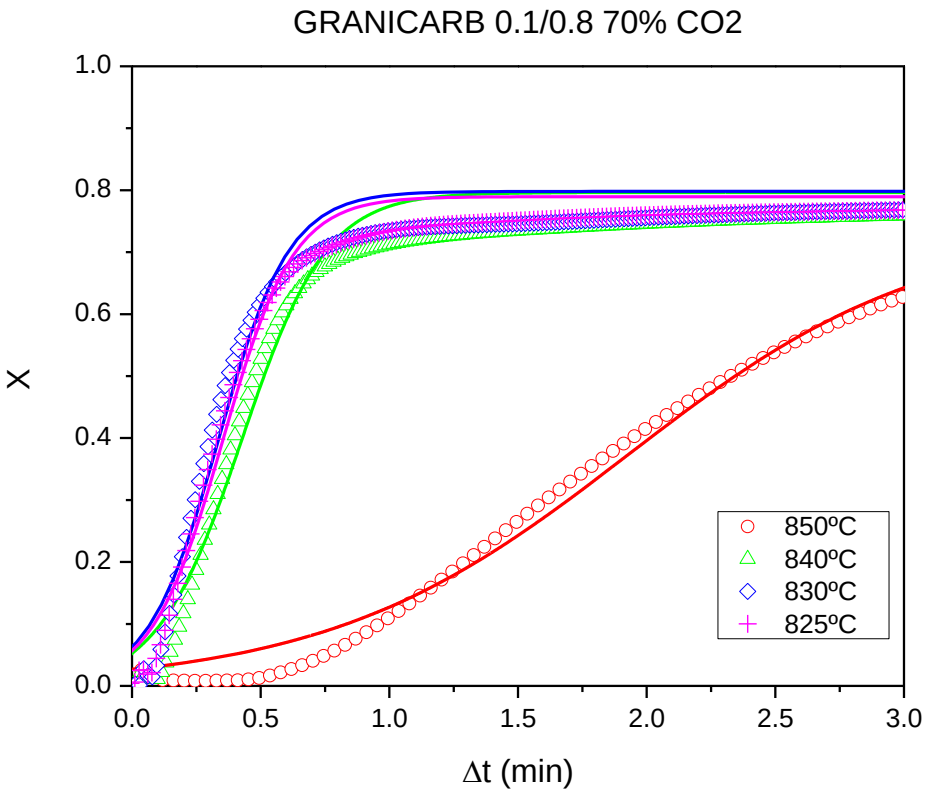

Figure 16. – X vs time plot for GRANICARB 0.1/0.8 carbonated at 825°C, 830°C, 840°C and 850°C under 70%vol. CO_2. The symbols correspond to experimental data and the solid lines correspond to the fit to equation 9.

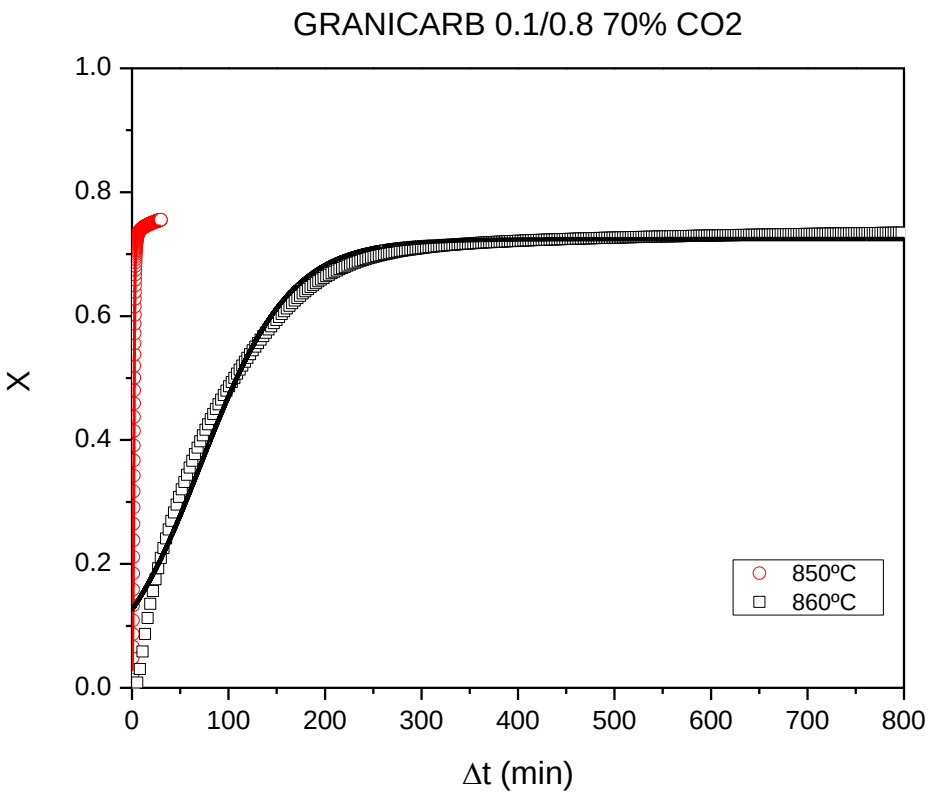

Figure 17. – X vs time plot for GRANICARB 0.1/0.8 carbonated at 850°C and 860°C under 70%vol. CO_2. The symbols correspond to experimental data and the solid lines correspond to the fit to equation 9.

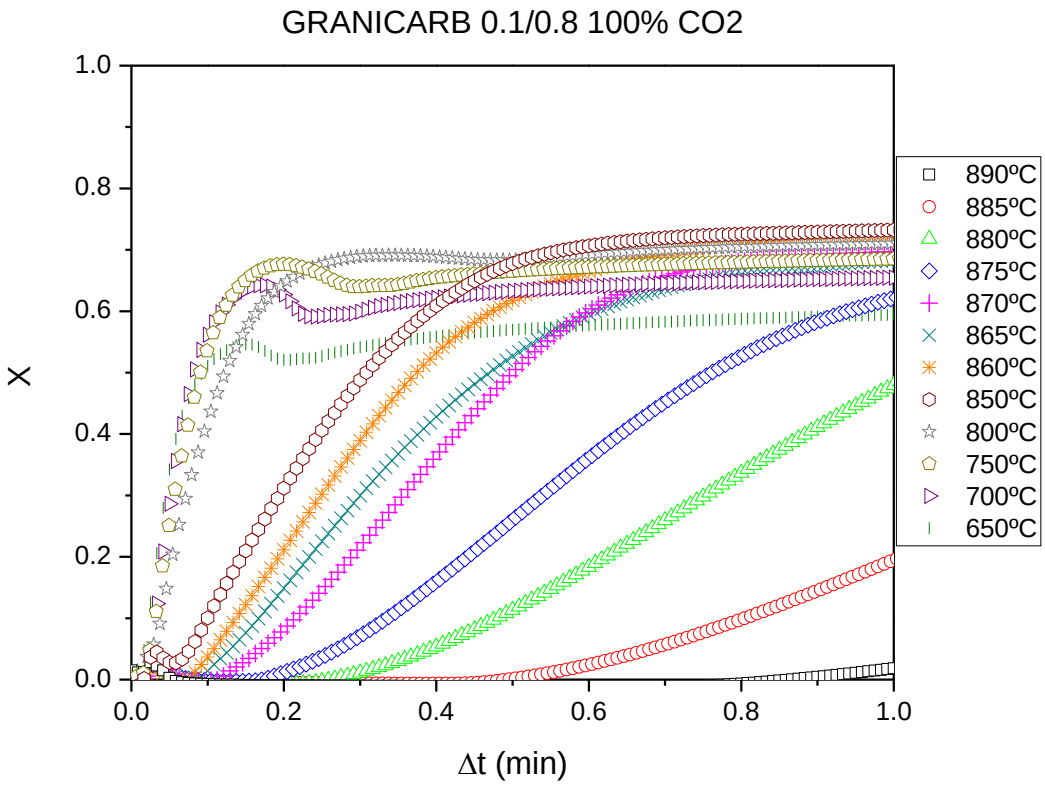

Figure 18. – X vs time plot for GRANICARB 0.1/0.8. Carbonation was performed at different temperatures under pure CO_2.

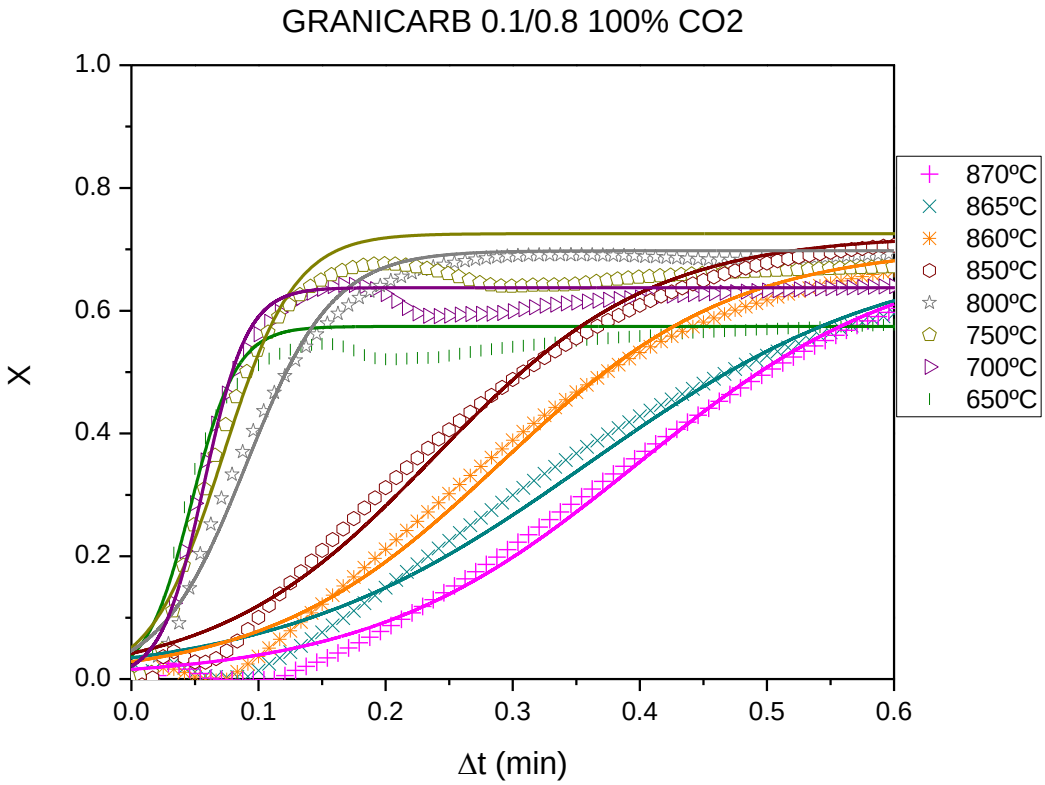

Figure 19. – X vs time plot for GRANICARB 0.1/0.8 carbonated at different temperatures between 650°C and 870°C under pure CO_2. The symbols correspond to experimental data and the solid lines correspond to the fit to equation 9.

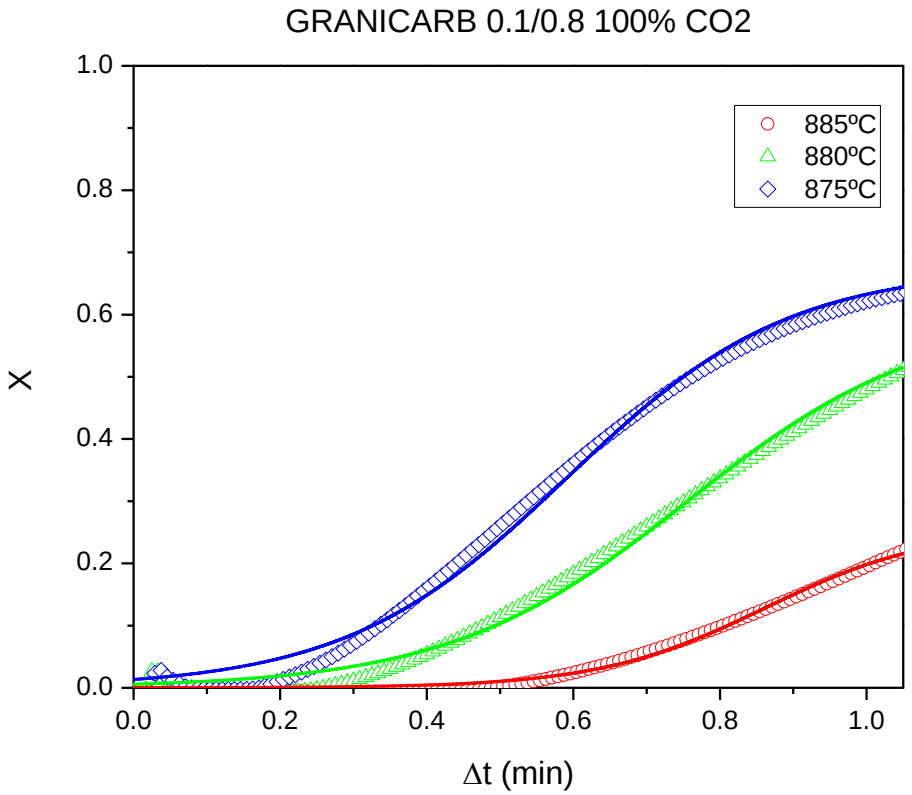

Figure 20. – X vs time plot for GRANICARB 0.1/0.8 carbonated at 875°C, 880°C and 885°C under pure CO_2. The symbols correspond to experimental data and the solid lines correspond to the fit to equation 9.

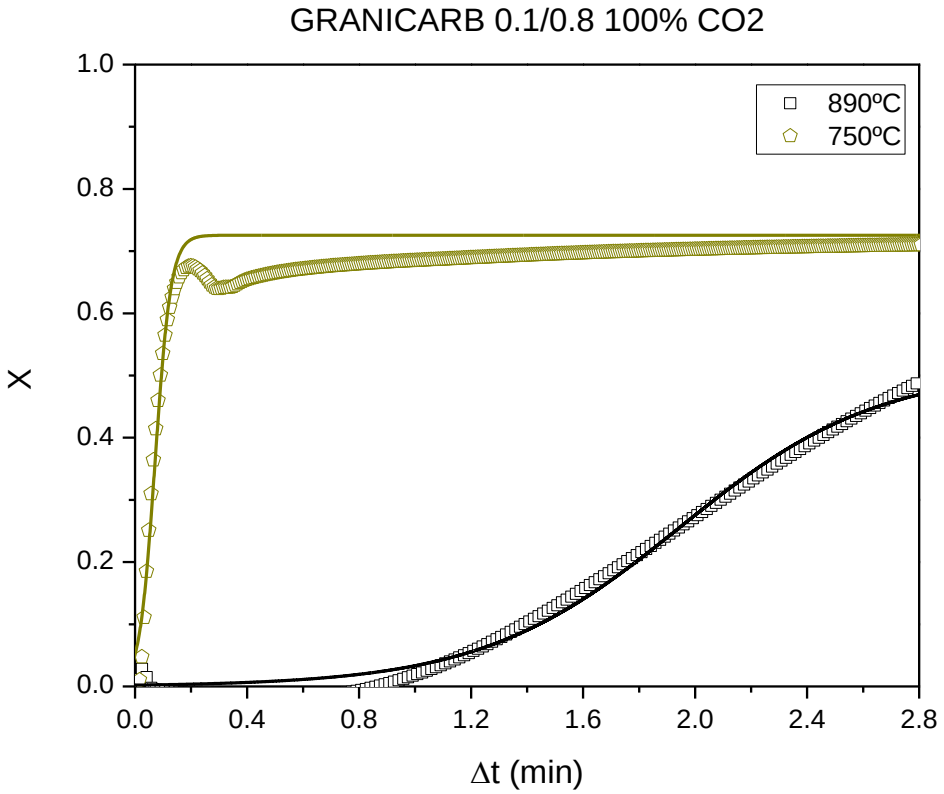

Figure 21. – Comparison of the X vs time plots for GRANICARB 0.1/0.8 carbonated at 750°C and 890°C under pure CO_2. The symbols correspond to experimental data and the solid lines correspond to the fit to equation 9.

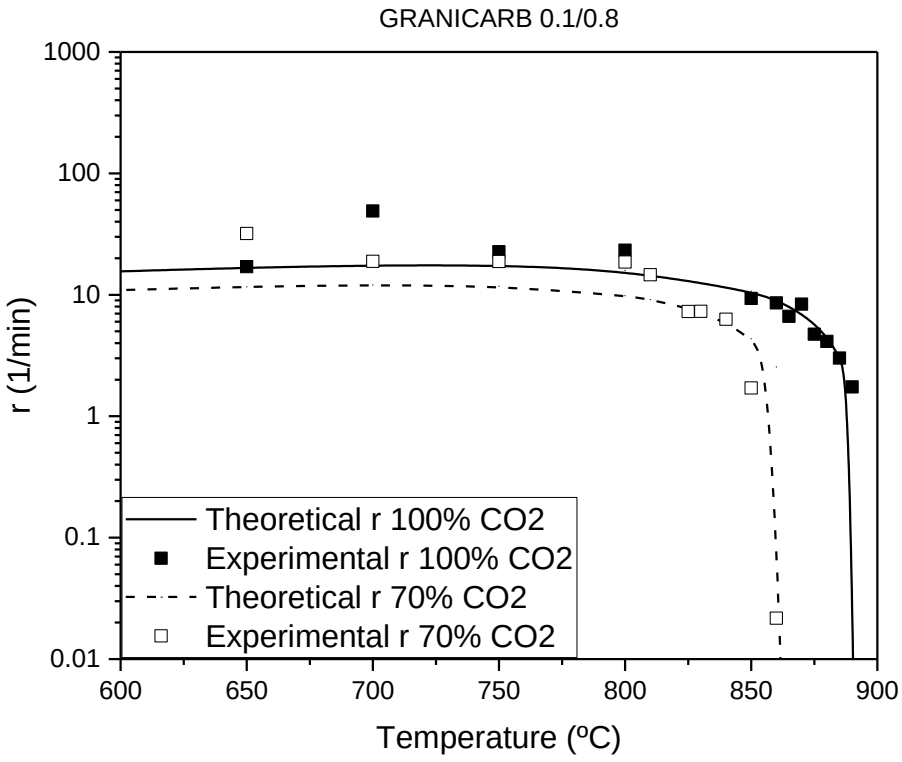

Figure 22. – Reaction rate values for GRANICARB 0.1/0.8 carbonated at different temperatures under 70% vol. CO_2 and pure CO_2. Solid lines correspond to reaction rate values obtained by applying the model (equation 5). The symbols correspond to the reaction rate values obtained by the fit of the X vs time plots to equation 9.

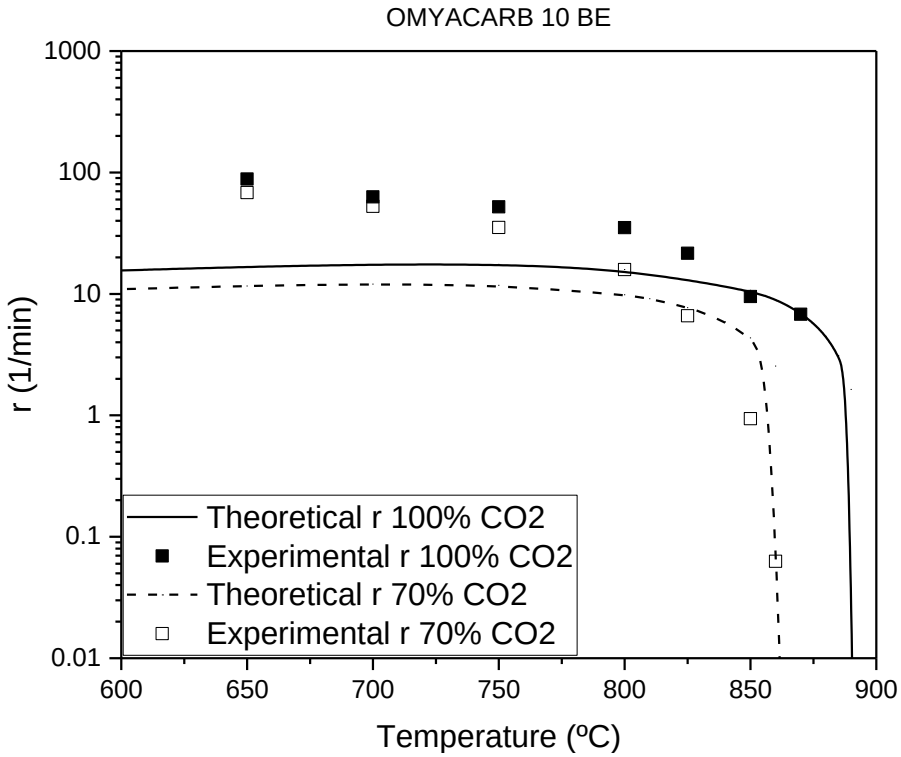

Figure 23. – Reaction rate values for OMYACARB 10 BE carbonated at different temperatures under 70%vol. CO_2 and pure CO_2. Solid lines correspond to reaction rate values obtained applying the model (equation 5). The symbols correspond to the reaction rate values obtained by the fit of the X vs time plots to equation 9.

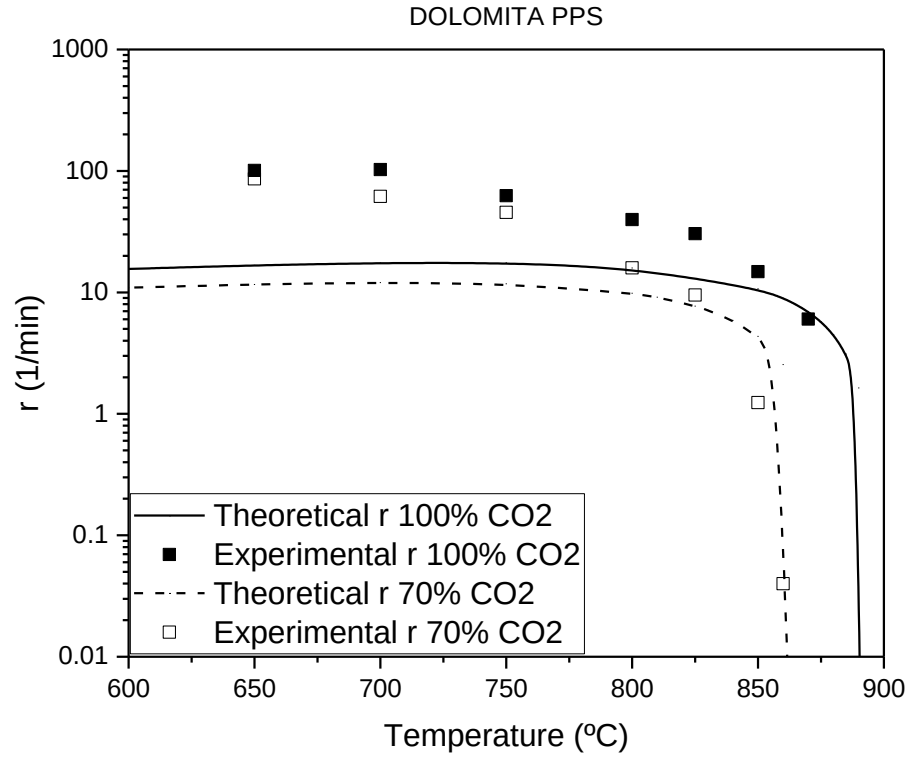

Figure 24. – Reaction rate values for DOLOMITA PPS carbonated at different temperatures under 70%vol. CO_2 and pure CO_2. Solid lines correspond to reaction rate values obtained applying the model (equation 5). The symbols correspond to the reaction rate values obtained by the fit of the X vs time plots to equation 9.

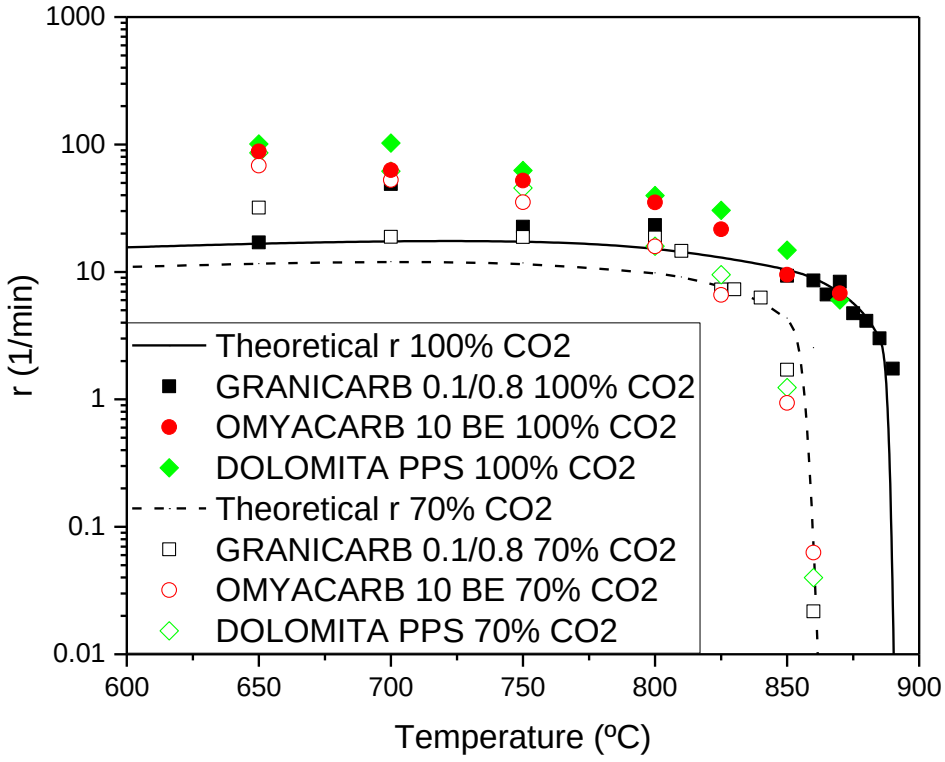

Figure 25. – Reaction rate values for all the studied samples, carbonated at different temperatures under 70%vol. CO_2 and pure CO_2. Solid lines correspond to reaction rate values obtained applying the model (equation 5). The symbols correspond to the reaction rate values obtained by the fit of the X vs time plots to equation 9.

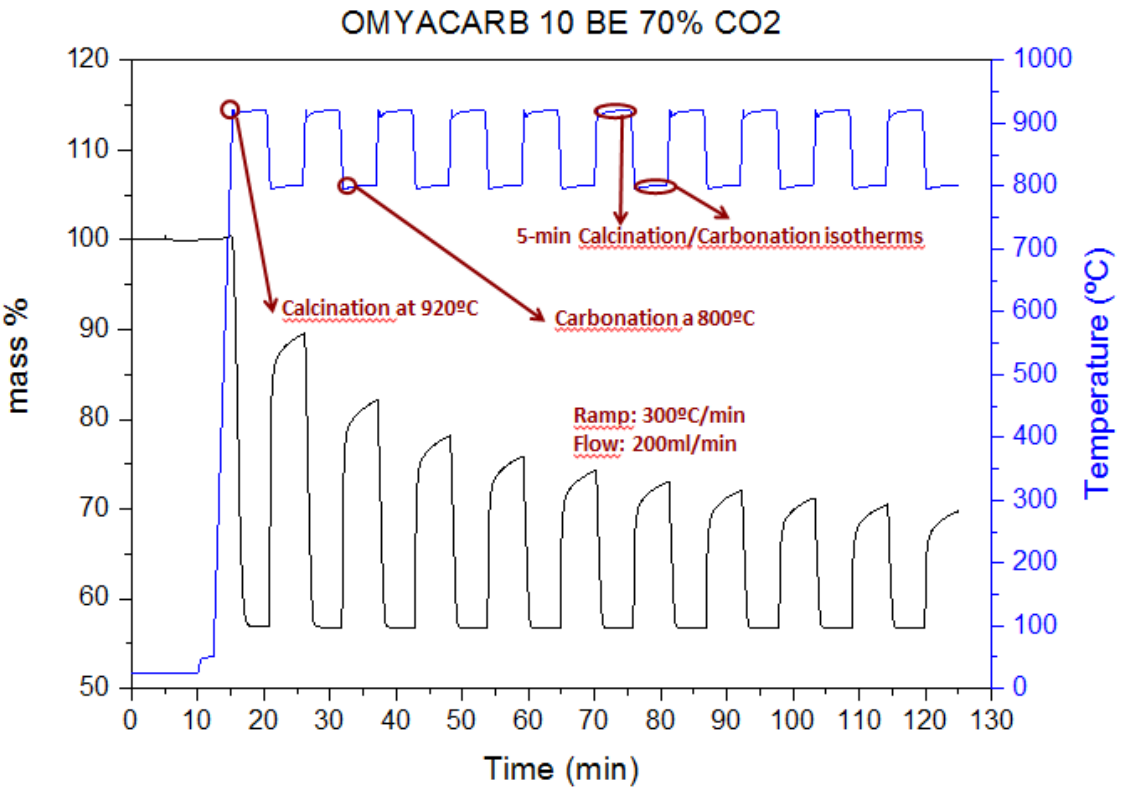

Figure 26. – Time evolution of temperature and sample mass% during calcination/carbonation cycles performed under 70%vol. CO_2 for OMYACARB 10 BE. Calcination at 920°C for 5 minutes and carbonation at 800°C for 5 minutes.

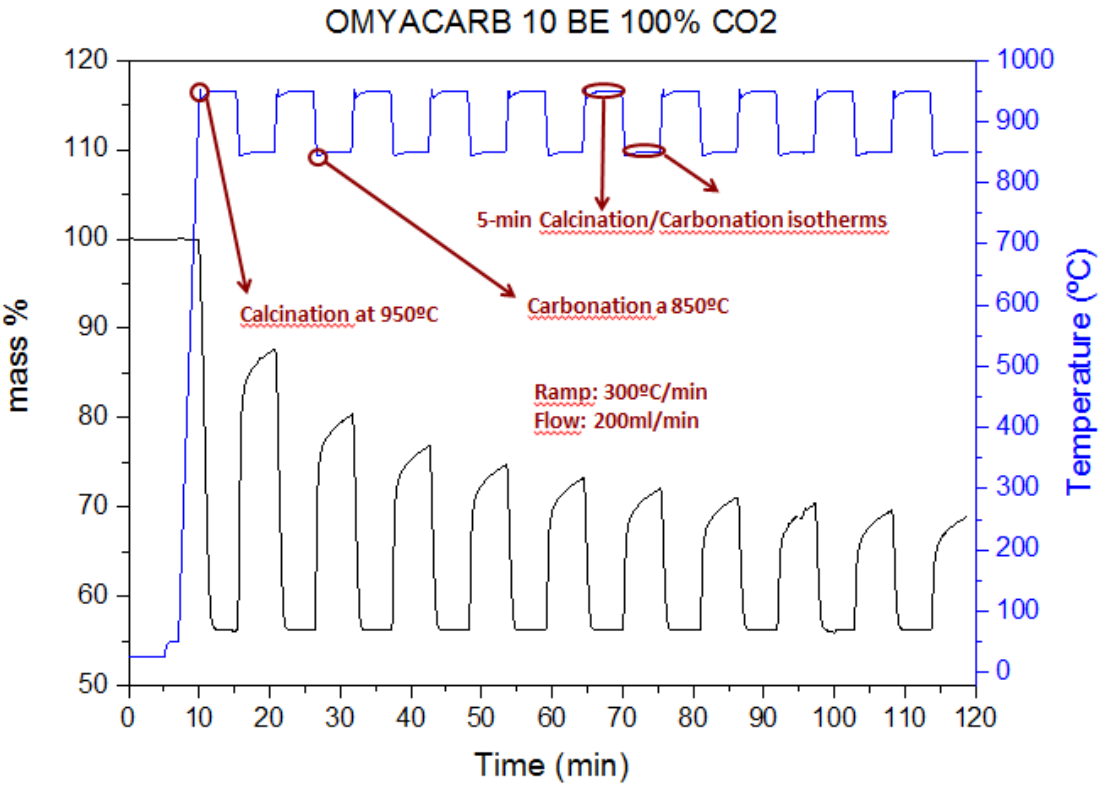

Figure 27. – Time evolution of temperature and sample mass% during calcination/carbonation cycles performed under pure CO_2 for for OMYACARB 10 BE. Calcination at 950°C for 5 minutes and carbonation at 850°C for 5 minutes.

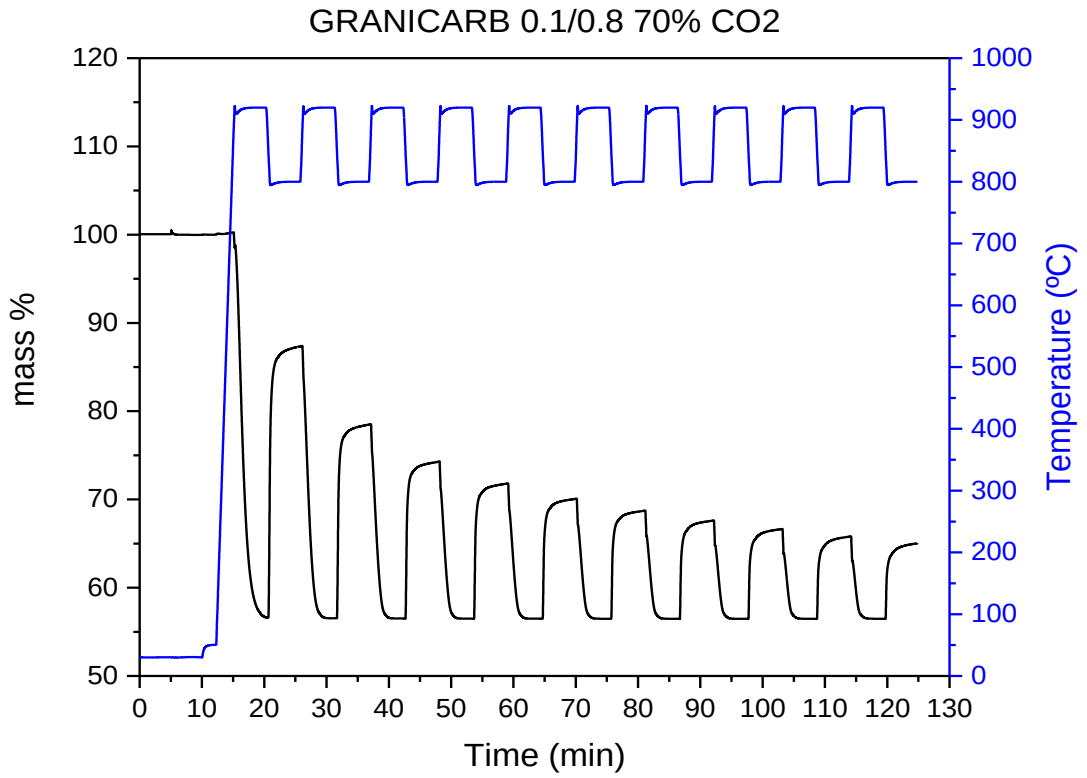

Figure 28. –Time evolution of temperature and sample mass% during calcination/carbonation cycles performed under 70%vol. CO_2 for GRANICARB 0.1/0.8. Calcination at 920°C for 5 minutes and carbonation at 800°C for 5 minutes.

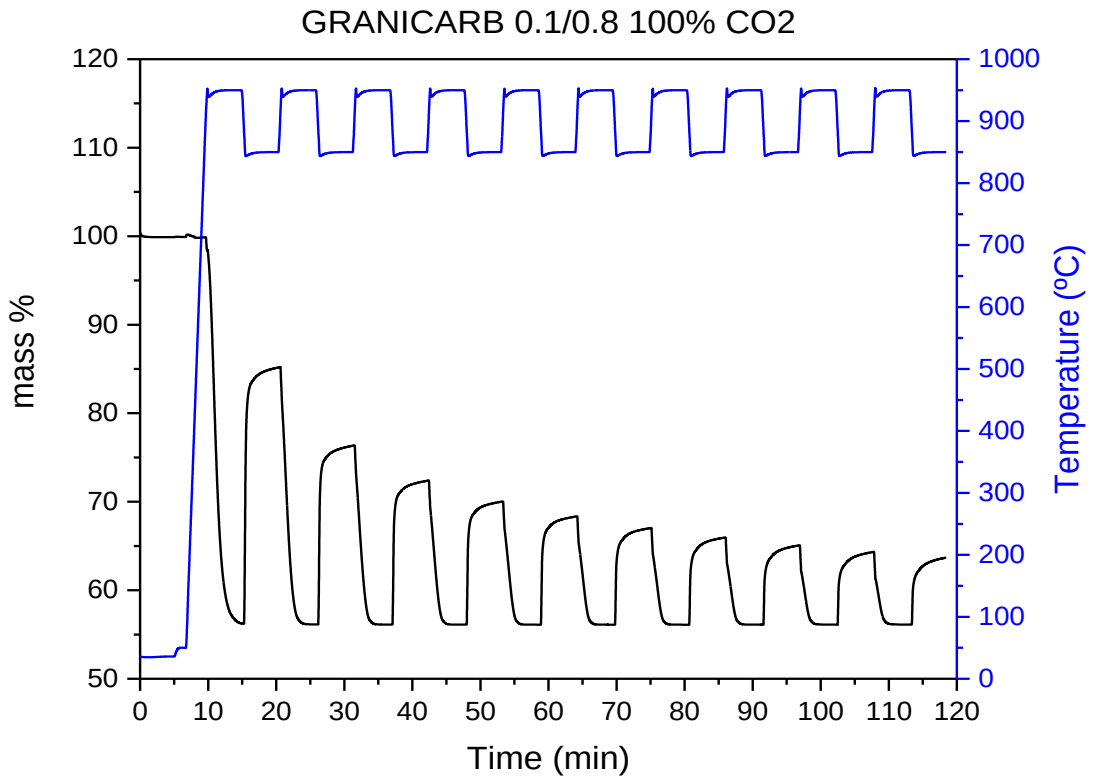

***Figure** 29. – Time evolution of temperature and sample mass% during calcination/carbonation cycles performed under pure CO_2 for GRANICARB 0.1/0.8. Calcination at 950°C for 5 minutes and carbonation at 850°C for 5 minutes.*

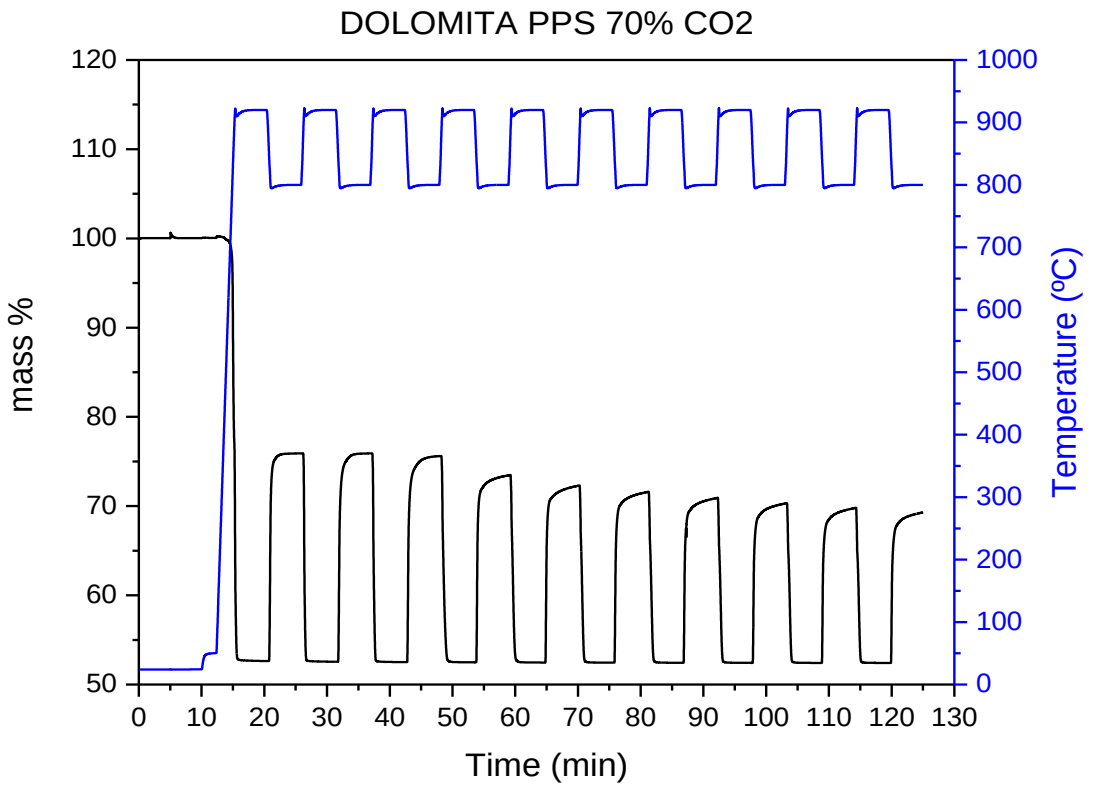

Figure 30. –Ttime evolution of temperature and sample mass% during calcination/carbonation cycles performed under 70%vol. CO_2 for DOLOMITA PPS. Calcination at 920°C for 5 minutes and carbonation at 800°C for 5 minutes.

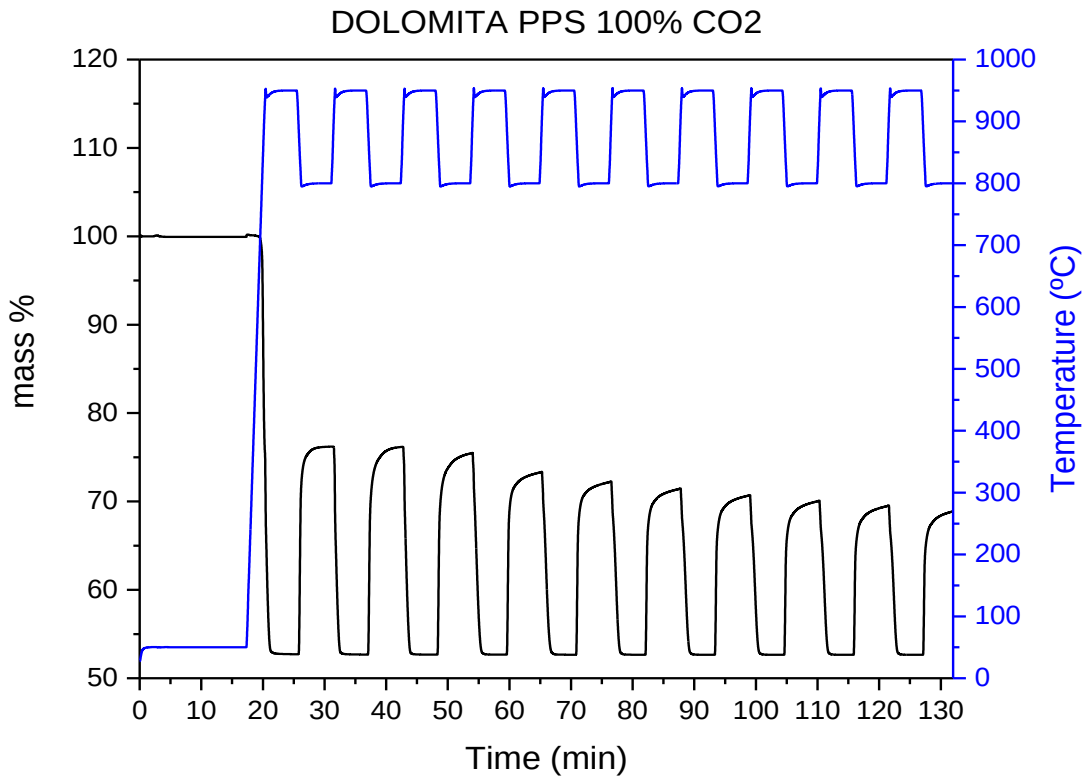

Figure 31. – Time evolution of temperature and sample mass% during calcination/carbonation cycles performed under pure CO_2 for DOLOMITA PPS. Calcination at 950°C for 5 minutes and carbonation at 850°C for 5 minutes.

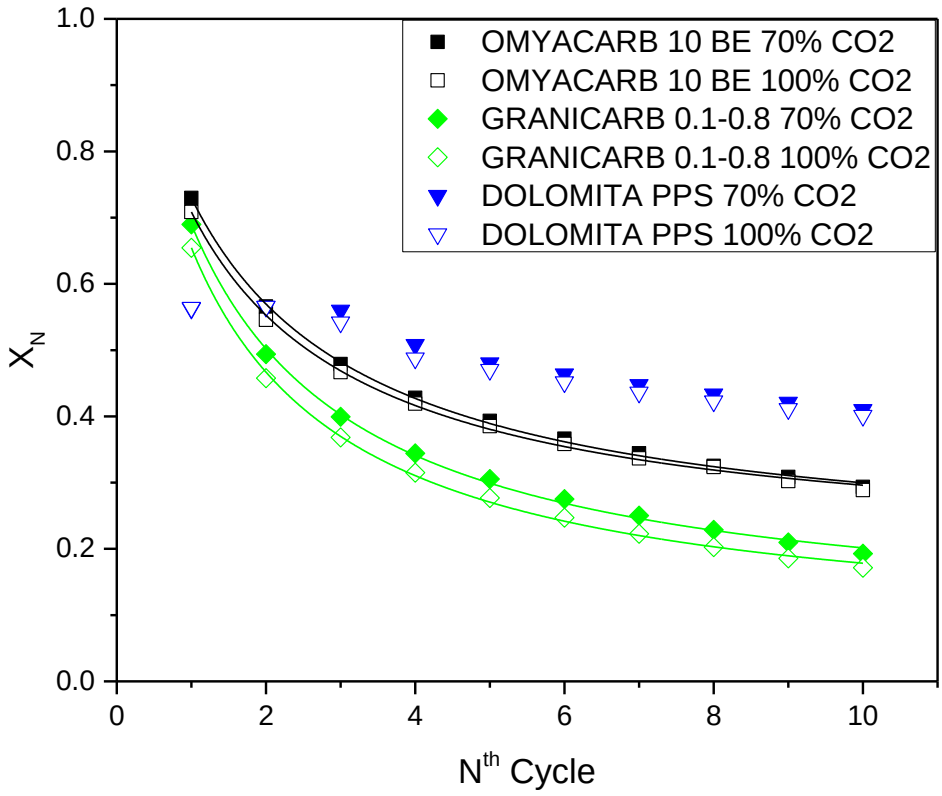

Figure 32. – Multicycle activity for all the samples cycled under 70%vol. CO_2 and pure CO_2. Solid lines correspond to the fit to equation 9. The symbolss correspond to the effective conversion of the samples at the N^{th} cycle calculated by equation 10.

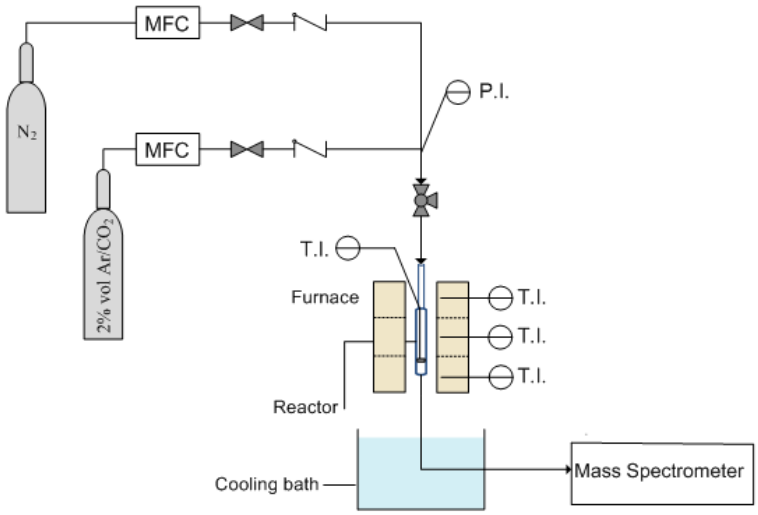

Figure 33. – Schematic diagram of the apparatus used for the kinetic experiments.

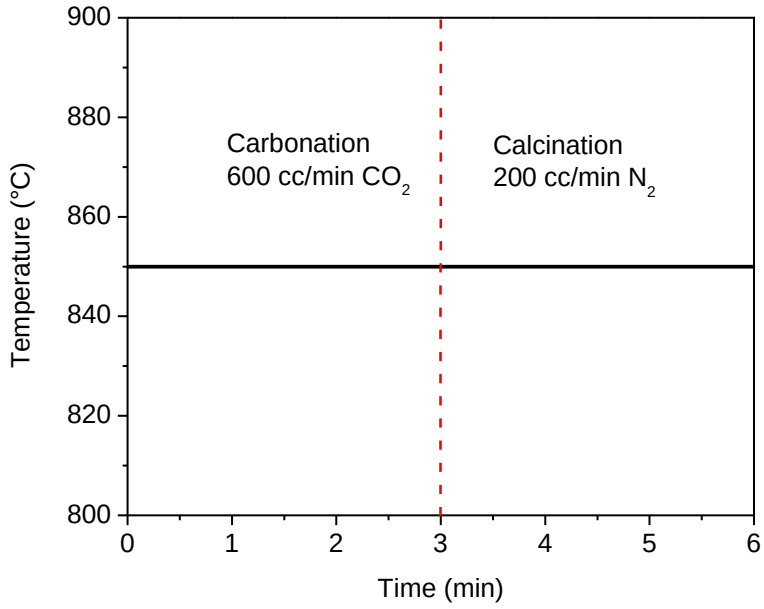

Figure 34. – Experimental protocol of the carbonation/calcination cycles during kinetics measurements (Carbonation: 850°C, 100%CO_2, 600ml/min).

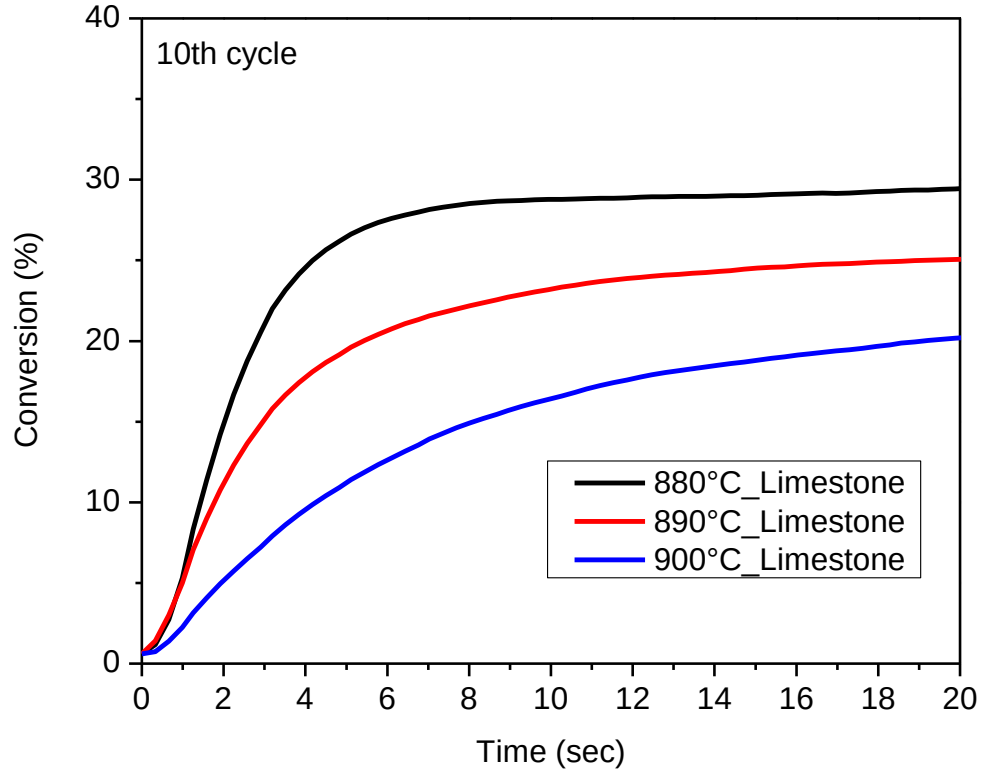

Figure 25. – Carbonation of limestone as a function of time for the three studied temperatures (<u>Material:</u> GRANICARB 0.1/0.8 (OMYA) (45-75 μm); <u>Carbonation</u>: 100%CO_2, 600ml/min, 3 min; <u>Calcination</u>: 100%/N_2, 200ml/min, 3 min; T=880, 890, 900°C, P=1.7 atm)

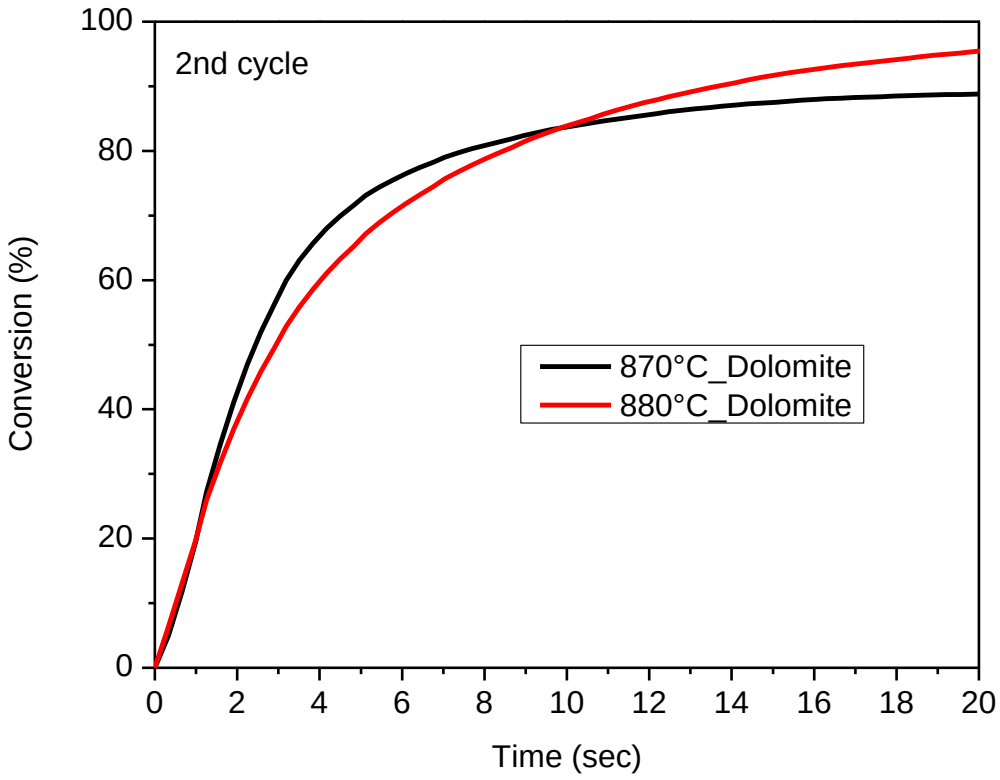

Figure 36. – Carbonation of dolomite as a function of time for the two studied temperatures (<u>Material:</u> MICRODOL 1-KN (OMYA) (45-75 μm); <u>Carbonation</u>: 100%CO_2, 600ml/min, 3 min; <u>Calcination</u>: 20 %CO_2/N_2, 500ml/min, 3 min; T=870, 880°C, P=1.7 atm)

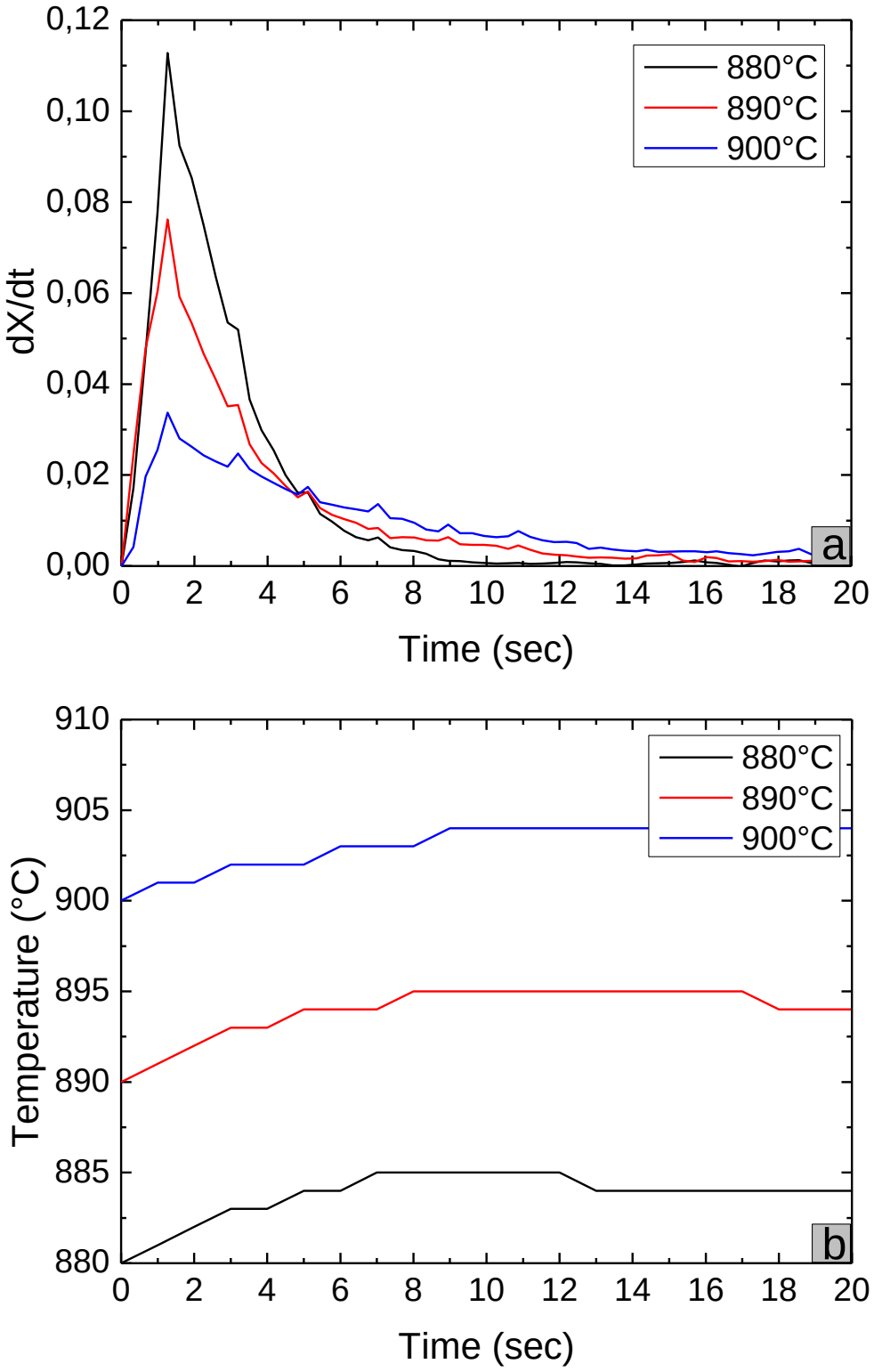

Figure 37. – Carbonation rate (a) and reactor's temperature profiles (b) for the three studied temperatures during the 10th cycle (<u>Material:</u> GRANICARB 0.1/0.8 (OMYA) (45-75 µm); <u>Carbonation</u>: 100%CO_2, 600ml/min, 3 min; <u>Calcination</u>: 100%/N_2, 200ml/min, 3 min; T=880, 890, 900°C, P=1.7 atm)

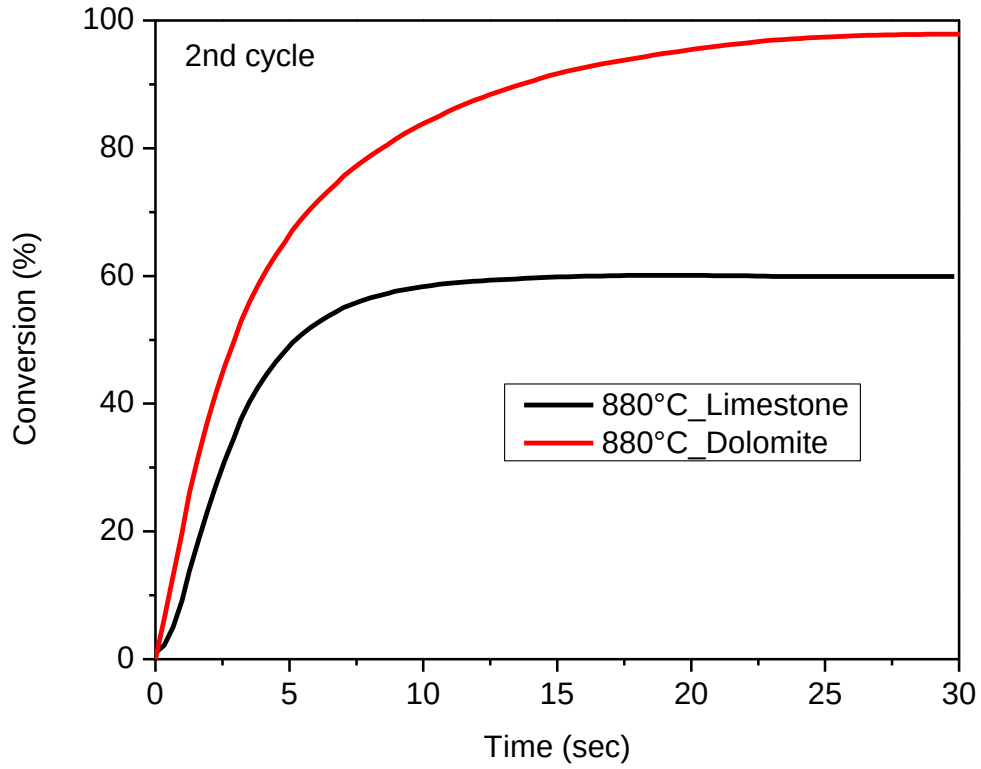

Figure 38. – Carbonation of limestone and dolomite at 880°C. <u>Materials</u>: GRANICARB 0.1/0.8 (OMYA) (45-75 µm), MICRODOL 1-KN (OMYA) (45-75 µm), sample mass: 100 mg. Carbonation conditions: gas flow: 600 cc/min (100 % CO_2). Calcination conditions: Temperature: 880°C, gas flow: 500 cc/min (20% CO_2 in N_2)

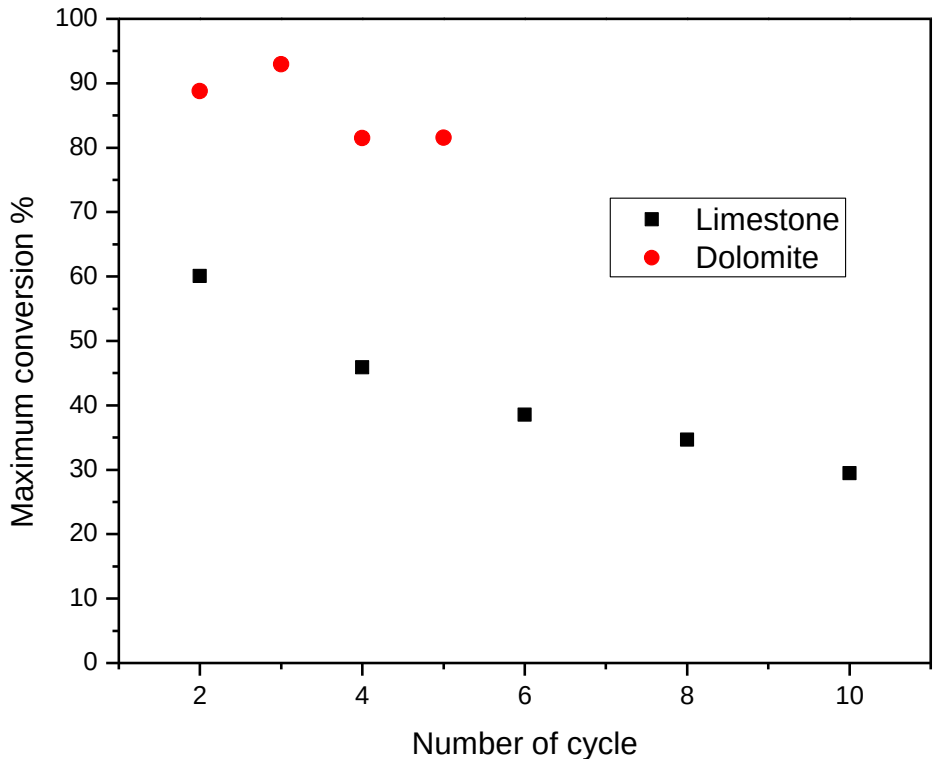

Figure 39. – Evolution of maximum conversion of limestone and dolomite through the cycles. Materials: GRANICARB 0.1/0.8 (OMYA) (45-75 µm), MICRODOL 1-KN (OMYA) (45-75 µm), sample mass: 100 mg., Calcination conditions: Temperature: 880°C, gas flow: 500 cc/min (20 % CO_2 in N_2), Carbonation conditions: Temperature: 880°C, gas flow: 600 cc/min CO_2

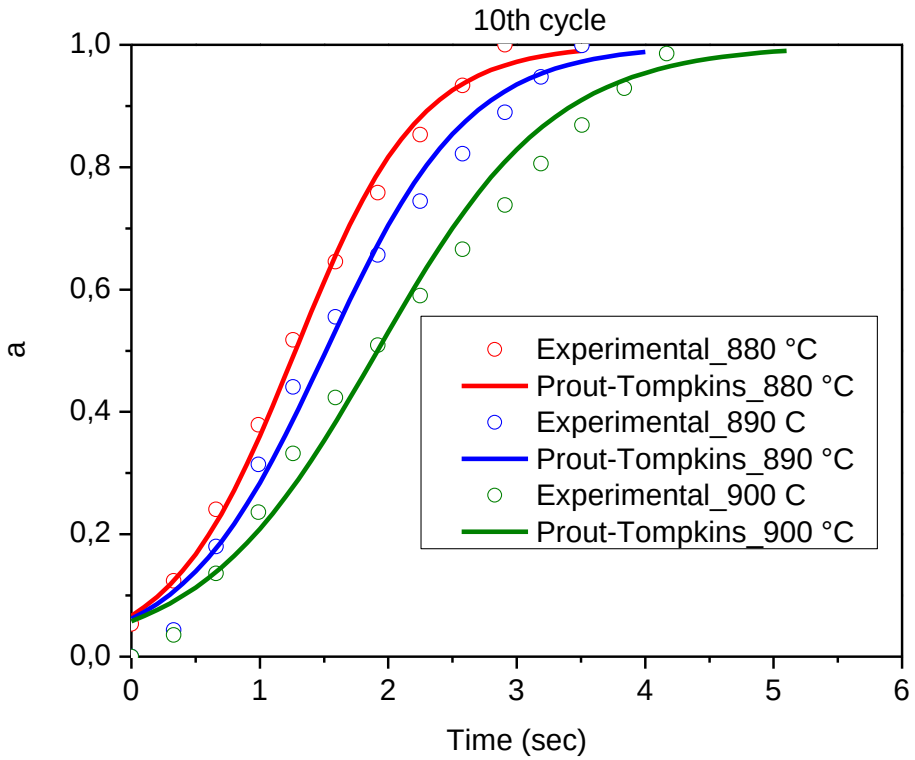

Figure 40. – Experimental carbonation conversion (normalized) during kinetically controlled regime as a function of time for the three studied temperatures and fit curves by the equation 9. (<u>Material:</u> GRANICARB 0.1/0.8 (OMYA) (45-75 µm); <u>Carbonation</u>: 100%CO_2, 600ml/min, 3 min; <u>Calcination</u>: 100%/N_2, 200ml/min, 3 min; T=880, 890, 900°C, P=1.7 atm)

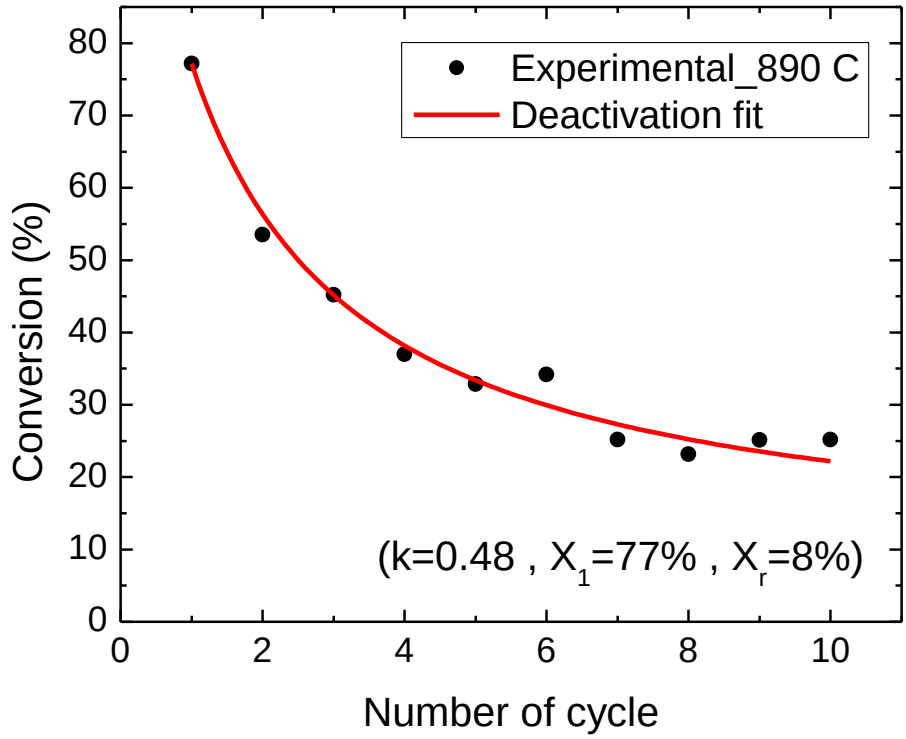

Figure 41. – Experimental carbonation conversion as a function of number of cycle and deactivation fit on equation 10 (<u>Material</u>: GRANICARB 0.1/0.8 (OMYA) (45-75 µm) <u>Carbonation</u>: 100%CO_2, 600ml/min, 3 min; <u>Calcination</u>: 100%/N_2, 200ml/min, 3 min; T=890°C, P=1.7 atm)

5. REFERENCES

1. W. J. Moore, *Physical Chemistry (5th Edition),* Prentice-Hall, 1999.
2. M. Benitez-Guerrero, J. M. Valverde, P. E. Sanchez-Jimenez, A. Perejon and L. A. Perez-Maqueda, "*Multicycle activity of natural CaCO3 minerals for thermochemical energy storage in Concentrated Solar Power plants,"* Sol. Energy, vol. 153, pp. 188-199, 2017
3. M. Benitez-Guerreroa, J. M. Valverde, P. E. Sanchez-Jimenez, A. Perejon and L. A. Perez-Maqueda, "*Calcium-Looping performance of mechanically modified Al2O3-CaO composites for energy storage and CO2 capture,"* Chem. Eng. J., vol. 334, pp. 2343–2355, 2018.
4. M. Benitez-Guerrero, B. Sarrion, A. Perejon, P. E. Sanchez-Jimenez, L. A.Perez-Maqueda and J. M. Valverde, "*Large-scale high-temperature solar energy storage using natural minerals,"* Sol. Ener. Mat.Sol. C., vol. 168, pp. 14-21, 2017.
5. M. Benitez-Guerrero, J. M. Valverde, A. Perejon, P. E. Sanchez-Jimenez and L. A. Perez-Maqueda, "*Low-cost Ca-based composites synthesized by biotemplate method for thermochemical energy storage of concentrated solar power,"* Appl. Energy, vol. 210, pp. 108-116, 2018.6. P. Sun, J. Grace., J. C. Lim, E. Anthony, "*The effect of CaO sintering on cyclic CO2 capture in energy systems,"* AIChE J., vol. 53, pp. 2432-2442, 2007.
7. D. Beruto, L. Barco and A. W. Searcy, "*CO2-catalyzed surface area and po-rosity changes in high-surface area CaO aggregates,"* J. Am. Ceram. Soc.,vol. 67, pp. 512–515, 1984.
8. M. Pijolat, and L. Favergeon, *Kinetics and Mechanisms of Solid-Gas Reactions*, in *Handbook of Thermal Analysis and Calorimetry*, S. Vyazovkin, N. Koga, and C. Schick, Editors. Elsevier Science B.V., 2018
9. C. Ortiz, J. M. Valverde, R. Chacartegui and L. A. Perez-Maqueda "*Carbonation of Limestone Derived CaO for Thermochemical Energy Storage: From Kinetics to Process Integration in Concentrating Solar Plants,"* ACS Sustainable Chem. Eng., vol. 6, pp. 6404-6417, 2018.
10. A. S. Negi and S. C. Anand, *A Textbook of Physical Chemistry*, vol. 90, no. 11. Wiley-VCH Verlag GmbH & Co. KGaA, Weinheim, 1986.
11. C. T. Campbell and J. R. V. Sellers, "*The Entropies of Adsorbed Molecules,"* J. Am. Chem. Soc., vol.134, pp. 18109-18115, 2012.
12. J. M. Criado, M. Gonzalez, J. Malek and A. Ortega, "*The effect of the CO2 pressure on the thermal decomposition kinetics of calcium carbonate,"* Thermochimica Acta, vol. 254, pp. 121-127, 1995.
13. A. Khawam and D. R. Flanagan, "*Solid-State Kinetic Models: Basics and Mathematical Fundamentals,"* J. Phys. Chem. B., vol. 110**,** pp. 17315-17328, 2006.
14. M. E. Brown, "*The Prout-Tompkins rate equation in solid-state kinetics,"* Thermochimica Acta, vol. 300, pp. 93-106, 1997.
15. J. M. Valverde, "*A model on the CaO multicyclic conversion in the Ca-looping proces,"* Chem. Eng. J., vol. 228, pp. 1195-1206, 2013.

CONCLUSIONS

The kinetics of carbonation of two limestones (GRANICARB 0.1/0.8 and OMYACARB 10 BE) and one dolomite (DOLOMITA PPS) has been studied by CSIC using thermogravimetry. Thus, carbonation was carried out at different temperatures under pure CO_2 and 70%vol.CO_2:30%vol. He atmosphere. It is observed that for a given temperature, carbonation rate increases as particle size decreases for the limestones. Moreover, carbonation rates of dolomite are higher than the calculated for the limestones. The results obtained by AUTH suggest that carbonation of CaO can proceed at high rates in a pure CO_2 stream when temperatures in the range of 880-900°C are applied and an operating pressure slightly higher than atmospheric (1.7 atm).

Due to equilibrium constrains, for a given sample at the same temperature, the carbonation rate is higher if the CO_2 partial pressure is increased.

For the carbonation experiments carried out at temperatures far from equilibrium (650-800°C) an overshoot in the mass signal is observed. This effect is attributed to the very fast carbonation reaction that takes place at these temperatures. Anyway, the model predicts reasonably well the experimental results, as shown in Figures 22-25, especially at temperatures near the equilibrium. The P-T model also describes adequately the evolution of conversion during the kinetically controlled regime for AUTH experiments. The obtained value of the pre-exponential factor a_2 (≈75000 s^{-1}) is much higher showing the high reaction rate when carbonation is conducted under efficient gas-solid reaction conditions (e.g. fixed or fluid bed reactors).

Regarding the multicycle activity of the two limestones and the dolomites, the effective conversion decreases with the cycle number due to CaO sintering. This effect is more pronounced for the limestones than for the dolomite since the presence of MgO grains in dolomite after the first calcination hinders CaO sintering. From X_1, X_R and k values obtained by the fits of the effective conversions to equation 9 (Table 4), it can be stablished that the effect of particle size on CO_2 uptake is much more relevant than that of the experimental conditions employed to perform the calcination/carbonation cycles.

As a general conclusion, it can be said that under SOCRATCES conditions, the reaction rates are quite large. The proposed model seems to fit the carbonation reaction with just some deviations for low temperatures experiments due, probably, to the difficulties in controlling the temperature in the experiments because of the exothermicity of the process. In any case, the experimental rates are above those predicted by the model.

Future plans include also studying the effect of steam addition at low concentrations (5-10 vol.%) and the evaluation of different mathematic models for carbonation kinetics. Moreover, the kinetics of calcination step are studied separately in WP3, which in addition to the obtained results in this WP will contribute to the design of the concept.